Master Erasmus Mundus in
Color in Informatics and Media Technology (CIMET)

Spectral Print Reproduction - Modeling and Feasibility

Master Thesis Report

Presented by

Kristina Marijanovic

and defended at

Gjøvik University College

Academic Supervisor(s): prof.Jon Yngve Hardeberg

Jury Committee: Eva Valero - University of Granada, Spain
Joni Orava - University of Eastern Finland

Spectral Print Reproduction - Modeling and Feasibility

Kristina Marijanovic

2012/07/15

Abstract

Towards the goal of spectral print reproduction a few obstacles can be found comparing to reproduction of colorimetric match. Human visual system is able to sense wide spectrum of colors and placing that range on substrate, weather paper or any other, requires skills. Traditional printing reproduction is built on metamerism phenomena and now the new challenge to overcome that constraint is set. To create the communication with print mechanism is very important and for that reason spectral printer modeling represents the crucial step. With this process characterization of the printer is done. This depends on the data given and optimal way of its use needs to be established. With forward printer model the relation between the colorant combination and the resulting spectral reflectances printed on substrate is defined. The inverse process enables printer control to define the colorant separation from spectral refelectances to precise values. Very important step in the whole process is not only measuring the printed material but overcoming time and resources waste with estimating spectral reflectances and combining them with already measured ones. Several models were tested by now and our contribution is consisted of employing Kubelka-Munk theory for estimation step before testing it with cellular model that makes printed cell smaller than unity and therefore more precise. Among the rest possible theories for estimation Kubelka-Munk theory was chosen due to its consideration of light scattering. This was mainly because the study samples used for spectral reproduction were garnament products. Before the target spectral reflectances values can be printed the feasibility of the process should be considered. Possibility for making that process as much automated as it can be was the main motivation in creation of feasibility of spectral reproduction algorithm.

Preface

I would like to thank you my supervisor, professor Jon Yngve Hardeberg, for not only academic support but for constant inspiration and all the question marks created above my head after Monday meetings. Thank you. Next I would like to thank all the members of The Norwegian Colour and Visual Computing Laboratory, especially to Aditya Suneel Sole and Peter Nussbaum for their help in the lab as well as friendly talks and interest in my topic. My work on thesis would never be the same without my colleagues and CIMET friends with whom I have spent four amazing semesters. I thank you all guys for being always (t)here for me.

In the end I want to express my huge gratitude to my parents, Mirjana and Jure, for always respecting my freedom of choice and personal space. For this courage I will always admire you and being thankful to have you in my life.

I also want to thank to Norwegian weather for assuring me there is no such thing as impossible.

Contents

List of Figures

1 Introduction

Spectral print reproduction is challange of modern print world and within this master thesis work two main questions were aimed to be answered. Before any of those are stated it should be noted that in our work the target object to be spectraly print was ganament product. This is important because that fact requires scattering of light to be strongly considered.

1.1 Problem statement

Due to statment above the first part of thesis is a try to create the optimal characterisation process and model the printer spectrally. Not only measured spectral reflectances of the printed product was considered but the estimated and mixed measured and estimated reflectances as well. Prediction of the printed ramps is important to be as much precise due to computational manipulation of the data. It is not always possible to actually print out and measure all the combinations printed. This is due to the exponential problem that raises with number of colorants being increased. Taking into account importance of the scattering of light in garnament products the Kubelka-Munk theory was chosen to be employed for estimation of the spectral reflectances. The second part of the thesis work was dedicated to answering feasibility question. From the world that surrounds us human visual system is able to sense much wider range of color than any output system is able to reproduce. Printing machines are part of that system with their own defined environment and communication channels and the real challenge is these to be overcome. Certain data with different kind of sensors describes the objects, in our case that data is defined with the spectrophotometers. Before sending any data to printing process in order to obtain spectral print the feasibility of that process should be confirmed. If neglecting that fact, hit-and-miss tries would yield big waste of time and energy. For that reason the automated process in verifying the feasibility of color sensation being printed spectrally of certain object was aimed to be created.

1.2 Answer to the problem stated

In our work big part of experimental process was conducted with the spectral reflectances data of the garnament samples. This was result of collaboration with the retail store from the USA. The final goal of retailer is to have the color values obtained under certain condition (geometry, illuminants) produced on paper substrate in printed form. For the scattering importance of the material, the Kubelka-Munk was employed in very similar way as it was done by Assefa in [1] and Blahova in [2]. Within this thesis this was tried to be extended even more with testing not only basic spectral printer models but breaking the initial cell (unity) to smaller space. The process was started with Murray-Davies spectral print model from where inverse effective colorant coverage was obtained. Once the effective coverage was available the estimation of the Neuge-

bauer Primaries was done. Neugebauer Primaries are set of reflectances made of primaries of the printer and their possible combinations of full coverage plus the reflectance of the substrate (paper). Not only the measured and estimated reflectances were used in testing the models but also their combinations (mixed reflectances). The test was conducted for spectral Neugebauer model, Yule-Nielsen Spectral Neugebauer Model for two different printers and technologies. The new step and contribution was introducing the estimation with Kubelka-Munk to cellular version of mentioned models. That way the cellular spectral Neugebauer model and cellular Yule-Nielsen Spectral Neugebauer Model were prepared to be tested. Comparing to non-cellular spectral models cellular extention resulted with more accurate results.
In the second part of thesis where the challenge of spectral print feasibility of target object was tried to be automated, several different steps in creation of that process were created in one so that the new algorithm, which includes all the segments in one step that saves time, was proposed. In this way big amount of input data can be initially placed and from the output it can be seen exact which parts of the gamut for targeted spectral reproduction are missing. In this way the answer to set of the spectral print feasibility of number of objects, under the same illuminant, was given.

The thesis work was conducted with laser, inkjet and CrystalPoint (inkjet subset) printing technologies so the initial title of the master thesis 'Spectral modelling of multi-channel inkjet printer' was changed. This way the scope of research was extended to give opportunity as well to gamut area of spectral print reproduction.

2 Spectral printer models

2.1 Print reproduction

Print reproduction is taking advantage of subtractive color mixing. That is the kind of mixing where colored filters are illuminated with white light from behind, as illustrated in fig. 1. The commonly used subtractive primary colors are cyan, magenta and yellow. If all three are overlapped in effectively equal mixture all the light will be subtracted therefore giving black. Unlike this additive color mixing creates combination of red, green and blue light on the black background giving the white if all three overlap. Subtractive type of color mixing is characteristic for devices that use paints and pigments among as well are printers.

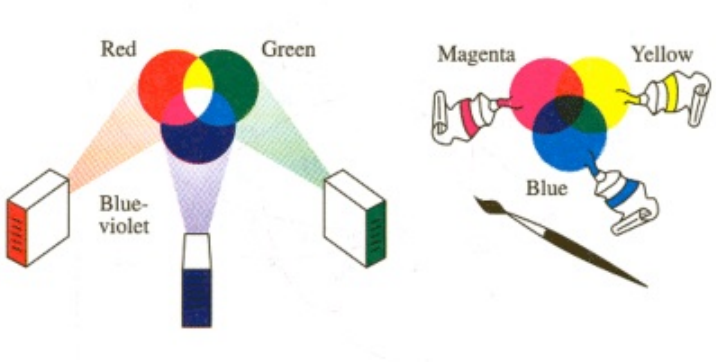

Figure 1: Additive color mixing represented on the left side versus subtractive color mixing on the right side of the figure.

2.2 Halftoning process

The process of creating screen dots, also known as halftoning [3] [4], converting continuous tone originals to printable elements that is suitable for printing reproduction. The screen dots are different sized and that, defending on their position, helps human eye to perceive continuous tone while observing the print. Depending on the printing process, there are usually only two states of ink transfer (printing or non-printing). This is why the varying visual impression of lightness or darkness must be created by varying the size of the halftone dot. If the screen structures are fine enough for the viewing distance of the screened image, the integrating effect of the human eye will in a way smooth out the image and the observer sees an image that, with it's continuous tone gradations, is visually consistent with the original. The greater the number of screen dots per image area, the more natural the effect of the image . The term screen ruling (or screen frequency) is used to define how close are the screen dots to each other [5] [6]. When

observing a 60 lines/cm screen (i.e., the screen frequency, usually referred to as the screen ruling L = 60 lines per cm, corresponding to a dot spacing w = 1/L = 0.167 mm) at a normal reading distance (approx. 30 cm), the eye is usually no longer able to detect the individual dots [**?**] [7]. With the help of the computer, the basic, manual screening process has been scientifically and mathematically analyzed in order to develop new, electronic reproduction processes. The basic principle of breaking down an image into different-sized screen dots which were equally spaced apart was initially preserved. The first systems capable of electronic screening were output scanners that imaged the films with very finely focused laser beams. The individual, different-sized dots were assembled from several laser spots (picture elements, pixels) [8] [9]. All laser image setters now work on this principle, first into the four basic colors (cyan,magenta, yellow, and black) of the printing process, and then into individual printing elements [10]. The screening of the individual color separations is done at different screen angles. This is necessary because the overprinting of different colors will occur without problems only using this procedure. Improper positioning of color separations causes interference, or so-called Moire patterns. Moire patterns can severely impair the image impression. This can be easily observed from figure 2.

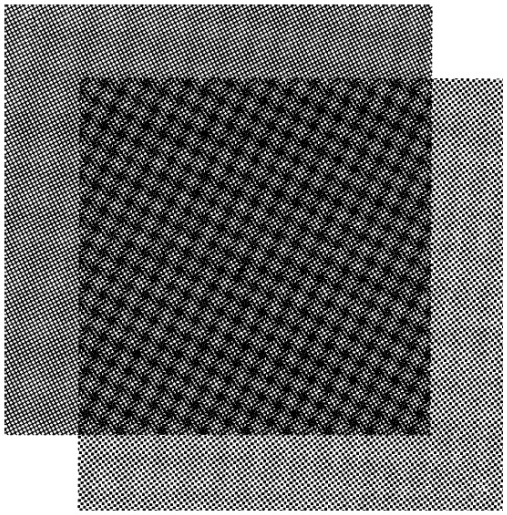

Figure 2: Moire effect created by interference through overlaying two periodic structures with similar screen angles - taken from [8].

With conventional reproduction technology, the color separations for the three chromatic colors were each offset at screen angles of 30 degrees in relation to each other.With four colors the least distinctive color, yellow, is output at an optimal angle of only 15 degrees in relation to magenta or cyan that is seen from figure 3.

Even if the optimal angle was formed when attempting to reduce interference effects/Moire phenomena, in homogeneous color areas rosettes may be formed as in figure 4.

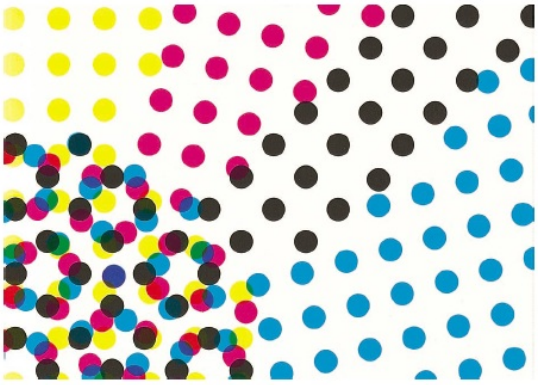

Figure 3: Angling of the screened color separations with rosette formation - taken from [8].

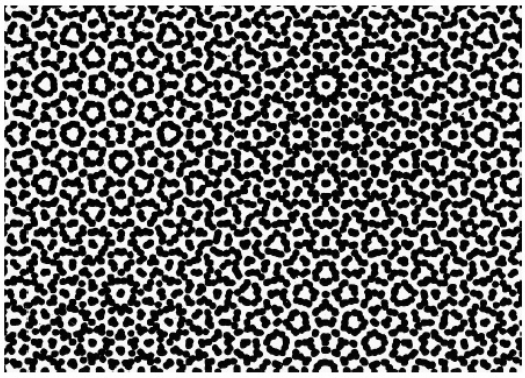

Figure 4: All color separations are printed with the same color so that Moire effect and rosettes created are easy to spot - taken from [8].

The formation of a rosette also depends on the relative positioning of the color separations to one another [8] [11]. Irregular rosette formation during printing can be caused by color register fluctuations. The finer the screen ruling, the less detectable the distorting structure. In printing technology most jobs make use of a screen ruling of about 60 lines/cm. Nevertheless, with originals having a distinctive, fine structure of their own (textile or filigree patterns, for example) structure-related Moire patterns may occur and are virtually unavoidable. Fine screens with up to 150 lines/cm are sometimes used for the reproduction of extremely fine structure details, even though they reduce Moire effects, they do not always prevent them [12]. In case of fine screens technical process-related requirements on reproduction technology and printing are exact imposed.

2.3 Murray-Davies model

Spectral printer model is a way to characterize printing process [13] [14]. With different models we are able to estimate the resulting spectral reflectances on the printing substrate for

any colorant combination. In the case of just one colorant print - monocolorant print, Murray-Davies model is fundamental equation for resulting spectral reflectance estimation. This model is regression-based model meaning that is relatively simple, with parameters fit to a set of data. It is useful for modeling printer output because it tends to be reasonably accurate and its simplicity allows for short calculation times [15]. Furthermore, having regression-based characteristics this model emulates the behavior of the system. By the assumptions of additivity inside a halftone cell, the spectral reflectance factor of a halftone cell printed on paper by a single colornat can be estimated based on the Murray-Davies equation [16]. In order to predict the reflectance of a single colorant coverage Murray-Davies model is employed for estimation of the spectral reflectance of a colorant coverage c as follows:

$$\hat{r}(\lambda) = (1 - c) \times r_{paper}(\lambda) + c \times r_{col,max}(\lambda) \tag{2.1}$$

where r_{paper} is the paper measured spectral reflectance, $r_{col,max}$ is the measured spectral reflectance of the paper covered by the colorant at maximum coverage. Usually $r_{col,max}$ value is 100% and $\hat{r}(\lambda)$ is the predicted spectral reflectance. Simple perform of linear interpolation between the reflectance of the paper and that of the full coverage colorant is result of Murray-Davies model. The estimated reflectance is the sum of the weighted reflectance of substrate and colorant where the weights are the distances along the line in colorant space. Estimated spectral reflectances obtained by Murray-Davies model assumes linear relation for each colorant printed on substrate. Linearity here denotes that for each primary the reflectance factors should be summed up according to their coverage dot areas. That is, if the coveragre (fraction) dot areas of a primary are summed up to a percent, from 0% to 100%, then the resultant reflectance factor is summed up to a percent of the reflectance factor of the primary at 100% area coverage. In physical print this relation is ruined and fails due to phenomena that limits linearity, this is known as dot-gain.

2.4 Dot gain

Dot gain is phenomenon that causes printed material to look darker than initially wanted [17] [18]. This is due to diameter of halftone dots which during printing process increases. Increase of the halftone dot placed on the substrate is caused by the optical and physical properties of the media and printer employed both in prepress and printing process. There are two sources of dot gain, mechanical and optical dot gain.

2.4.1 Mechanical dot gain

Mechanical dot gain is caused by printing ink submerging and spreading when delivered onto a paper substrate causing the physical dot size to be changed. This is due to the physical ink spread. A more fluid ink would spread more resulting in higher dot gain. Absorbance of the substrate also affects dot gain [19] [20]. Higher absorbance of the substrates is the higher is dot gain cause by easier spreading of the colorant through the paper substrate.

2.4.2 Optical dot gain

Optical dot gain comes from light flux that penetrates the colorant film, enters the paper substrate, scatters and finally emerges from non-ink area. In the same way light flux can enter the

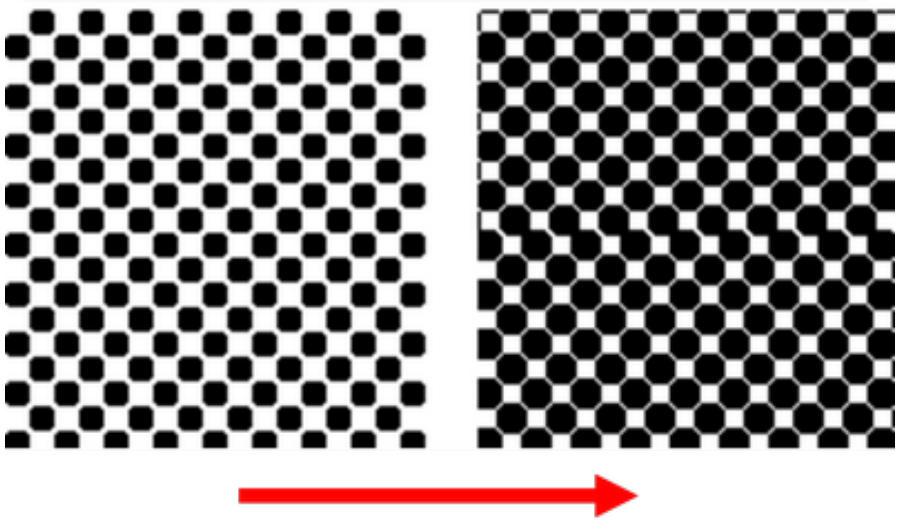

Figure 5: During printing process several phenomena occur that makes resulting printed dot bigger in size than initially wanted. Result of it is called dot-gain.

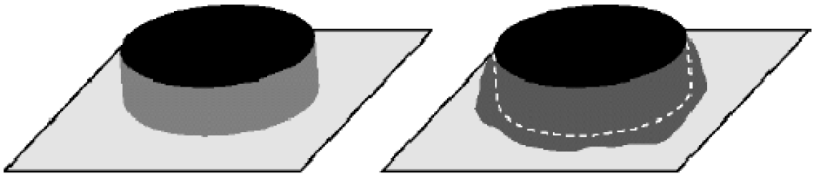

Figure 6: Mechanical dot gain occurs when printing ink is submerging and spreading when delivered on a paper substrate causing the physical dot size to be changed – taken from [21].

paper substrate and get scattered, penetrate the colorant film and finally emerge from there. This is basically resulted by the interaction of light with the colorant and paper. As the light penetrates the colorant on the way to the paper substrate, a certain amount of it is diffused. This diffused light may leave the edge of the placed colorant dot in different ways: to reflect light beyond physical dimensions of the placed dot or get trapped underneath the dot. In this way, even they are physical different, the dot appears bigger in size. These two physical phenomena are the reason for printing models having problem in prediction of dot size which has significant influence to estimated spectral reflectances.

2.5 Yule-Nielsen model

Towards better and more accurate printer modeling, dealing with both mechanical and optical dot-gain, n-factor was employed to modify initial Murray-Davies relation. This was introduced by Yule and Nielsen who worked on light penetration and scattering [22]. Their theoretical analysis showed that the nonlinear relationship between measured and predicted reflectance can be described with a power function. Starting from the base Murray-Davies model in equation 2.1

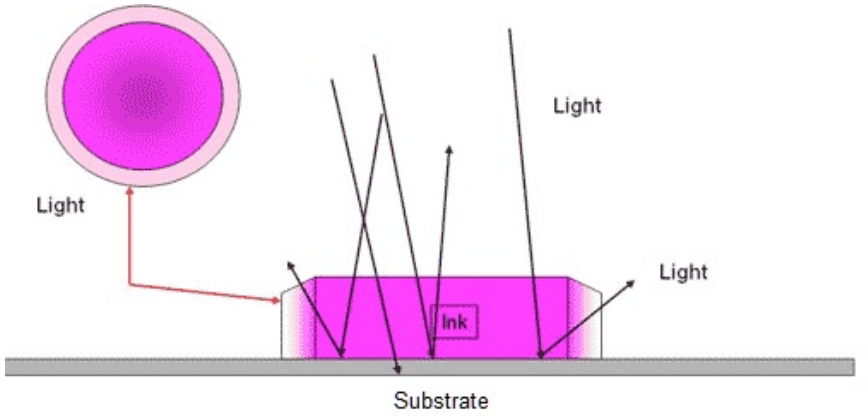

Figure 7: Optical dot occurs in the process of interaction of light with the ink and substrate.

they added the exponent $1/n$ to the reflectance values:

$$\hat{r}^{\frac{1}{n}}(\lambda) = (1-c) \times r_{paper}^{\frac{1}{n}}(\lambda) + c \times r_{col,max}^{\frac{1}{n}}(\lambda) \tag{2.2}$$

Even though their $n - factor$ is an empirical parameter through different research it was shown that it is capable to maintain high accuracy of model fitting. For this reason Yule-Nielsen $n - factor$ is still widely employed for its simplicity. In order to find the optimal n factor iterative process which estimates the spectral reflectances for various n factor values can be employed. Next, by comparing the estimated spectral reflectances with the measured spectral reflectances more information will be obtained so that the $n - value$ which gives the minimal colorimetric differences or smallest spectral difference can be chosen.

2.6 Dot areas

During the printing process paper substrate in close interaction with colorants results in different printed area than initially set up with digital values. This is mainly due to mechanical dot gain previously described in 2.4.1. Awareness of initial values being changed in final printed material is very important and distinction of those various types should be made. There are two different areas that are covered by colorant dots: theoretical area and effective area.

2.6.1 Theoretical area coverage

Theoretical area coverage is calculated from the actual binary image sent to the printer [23] [24]. While not always physically reasonable, a square pixel shape is assumed, and theoretical area coverage is determined as shown by the percentages. The simple way of describing theoretical coverage are pure numerical values or steps in ramp of a colorant. For instance, span from 0% to 100% coverage in step of 5% will result in ramp of 20 sub-patches. These values are always predeterminated and can be easy visualized i.e. with various test charts.

2.6.2 Effective area coverage

Opposite to that effective dot area (effective area coverage) is always an estimated value. For example, if the spectral reflectance is accurately predicted by a particular area coverage, this is referred to as the effective area coverage, a_{eff} . This is equivalent to selecting the best proportion such that it most closely matches the measured spectral reflectance at area coverage. It is important to establish relation between theoretical and effective area coverage [25]. This value can be obtained by calculating a_{eff} for each spectral reflectance measurement corresponding to a known theoretical colorant value sent to the printer. After being established, this relation is usually expressed in the form of a look-up table (LUT) for single colorant printing but can be, and in most of cases it is, performed for all the available colorants of a printing system.

2.7 Inverse Murray-Davies

Estimation of effective dot area can be done by modified use of the Murray Davies model. By rearranging 2.1 predicted effective dot area covered by the colorant of a known input value, which is in this case theoretical colorant coverage, can be found as follows:

$$a_{eff} = \frac{r_{\lambda=min,meas} - r_{\lambda=min,s}}{r_{\lambda=min,t} - r_{\lambda=min,s}} \tag{2.3}$$

It can be noticed that here $\hat{r}$ is replaced by the measured reflectance. Also, reflectance values are subscripted $\lambda = min$ that means this calculation is being performed at a single wavelength. a_{eff} can be seen as the factor by which the solid ink reflectance should be scaled to equal the measured reflectance of the sample. This equation is very important in fundamental stage of modeling because it can be used to estimate dot gain, therefore improving the estimation of area coverage. Since our data requires not only calculation with single reflectance but whole spectra range it should be extended to a spectral form. In order to that a_{eff} values needs be determined by a matrix calculation using least squares analysis:

$$a_{eff} = R_{meas,adj} R_{t,adj}^{T} (R_{t,adj} R_{t,adj}^{T})^{-1} \tag{2.4}$$

Reflectance terms in this equation are row vectors, the length of which is the number of wavelengths in the spectral measurement. Here, $R_{meas,adj} = R_{meas} - R_s$ and $R_{t,adj} = R_t - R_s$, and the superscipts T and -1 indicate matrix transpose and inverse [26] [27] . This calculation needs to be repeated for each patch in the separation ramp.

2.8 Spectral Neugebauer model

Apart for models being accurate as possible considering mechanical and optical dot gain tendency to developing one for not only monochrome but multicoloroant print was introduced by Hans E.J. Neugebauer in 1937. Neugebauer model considers all the channels of colorant of a printer and by extending initial Murray-Davies model gives a precise spectral reflectance value of possible combinations of colorants by taking into account 100% (full) colorant coverage [28]. By this model it is expressed that in case of k colorant printer (k number of channels) there will be 2^k Neugebauer Primaries(NPs). Set of printer's NP is created with spectral reflectances of full coverage of primaries (k), spectral reflectances of their full coverage overlaps and reflactances of

the paper substrate. Neugebauer computes the predicted reflectance vector $\hat{r}$ as the sum of each combination of colorants (NPs) weighted by their coverage and the spectral Neugebauer (SN) model can be then written as follows:

$$\hat{r}(\lambda) = \sum_{i=0}^{2^k-1} a_i R_i(\lambda) \tag{2.5}$$

where the summation over i represents the Nuegebauer Primaries: paper substrate, single colorants separations, and color overlaps; a_i is a scalar weighting representing the probability that a point on the page of the color mixture is covered by the i^{th} NP and $R_i(\lambda)$ is the reflectance vector of the primary. Not only for the full colorant coverage estimation of reflectances and resulting combination Neugebauer model was base for estimation the relative area of each primary. Relative area is the surface of the paper needed the most in everyday printing. It denotes all the steps on the way to reach full colorant coverage. Since it is not common that prints are made of just full colorant coverage this was important step. Towards the goal of estimating relative (fractional) colorant printed area Demichels model was employed.

2.9 Demichel model

The Demichel model is a statistical model that estimates the NP coverage for a given colorant combination. By this model it is assumed that the colorant coverage is statistically independent as well as placement between dots is independent. In our work the basic formulation of Demichel equation was used in extended version to four colorants. For the simplicity, and exponential problem that occurs with adding colorants, here is shown how Demichel equation works in basic, two colorant combination:

$$\begin{aligned} w_0 &= (1-c_1)(1-c_2) \\ w_1 &= c_1(1-c_2) \\ w_2 &= (1-c_1)c_2 \\ w_{12} &= c_1 c_2 \end{aligned} \tag{2.6}$$

where w_0 is the weight for the paper, since no colorant is placed on paper substrate. w_1 is the weight of the first colorant c_1, w_2 for colorant c_2 and w_{12} for the overlap of colorant c_1 and colorant c_2. It can be noted that in case of two colorants there will be 2^2 weights. For making the further calculation easier the obtained weights are represented in a vector form W as follows:

$$W = [w_0 w_1 w_2 w_{12}] \tag{2.7}$$

2.10 Yule-Nielsen Modified Spectral Neugebauer Model

Not only internal reflections in paper but other phenomena affects reflection spectrum of colorant being printed at paper substrate. As mentioned before the nonlinear relationship between the reflection spectra of paper and colorant placed was obtained empirically by Yule and Nielsen [29] [30] [31]. That was determinated by applying a power function, whose exponent n is fitted according to a limited set of measured patch reflection spectra. This non-linear relationship was

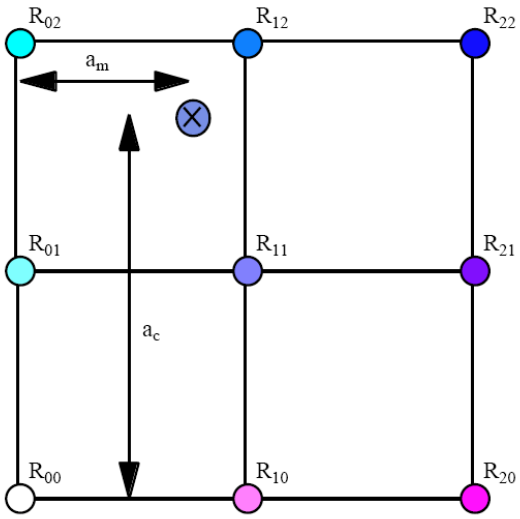

Figure 8: Example of cellular model where the reflectance of the test patch X is now calculated from the reflectance of R01, R02, R11, and R12 - from [34].

applied to the spectral Neugebauer model which resulted with more accurate model the Yule-Nielsen modified spectral Neugebauer (YNSN) model [32]:

$$\hat{r}(\lambda) = \sum_{i=0}^{2^k-1} (a_i R_i(\lambda)^{\frac{1}{n}})^n \tag{2.8}$$

Yule-Nielsen modified spectral Neugebauer model is still accurate and simple enough to prevent complex calculation in spectral estimation of print. It is important to note that when fitting $n - value$, effective area coverages must be calculated again and then put in the Demichel equations each time that $n - value$ is changed.

2.11 Cellular spectral Neugebauer Model

With spectral Neugebauer model the whole gamut of the printer has been achieved by interpolation from a few points on its surface [33]. This creates certain space of data. Taking into account spreading of the light as well as non-linear relationship it can be easily noted that interpolation of that data space would yield with result far away from accurate result. Besides applying the YuleNielsen n-value correction to deal with the nonlinearity and given actual area coverage effective area coverage there was another try in to creating that data space smaller. That approach is aiming to reduce the space over which interpolation is performed by providing more primaries that are inside the printer gamut. This can be done by measuring each colorant at 0, 50, and 100% area coverage so that the printer gamut is subdivided into smaller cells. This approach, because of dividing the initial gamut space into smaller cells, was called Cellular Neugebauer and was first presented by Heuberger et al.
Here a simplified case is presented graphically, with two divisions per separation, results in four cells for two-color printing. When using non-cellular Neugebauer, reflectance of the test patch,

marked with an X, is predicted by interpolating between R00, R02, R20, and R22 8. The use of cellular Neugebauer decreases the size of the interpolation cell [34]. The reflectance of the test patch is now calculated from the reflectance of R01, R02, R11, and R12 8. If more accuracy is required, more nods (primaries) can be added at the expense of computation and measurement time. When using cellular Neugebauer, the interpolation is identical to 2.5. However, additional computation is required to determine which primaries to use, or equivalently, selecting in which cell the interpolation is to be performed [35] [36]. This is an iterative process. Simiral to this, again search for rest colorant primaries is needed. With the identified cell, the effective area coverage of the colorant is calculated. Equations employed here are analog to 2.3 as well as the least square analysis form 2.4. They show the scalar form and the least squares analysis on the spectral reflectance data.
The main difference in terms relating to the cellular case involves following: adjusted values are those that have had the reflectance of the lower primary subtracted. So, here a_{eff} represents the effective colorant area coverage that is used to calculate the effective area coverages of the relevant Neugebauer primaries [37] [38]. This can be applied to predict spectral reflectance. What is also important to observe here is that cell boundaries do not need to be spaced uniformly. The best is to sample the space more frequently in areas where reflectance changes rapidly with respect to input area coverage but this depends on the particular printer used.

2.12 Cellular Yule-Nielsen spectral Neugebauer model

Another useful extension of the cellular case is the addition of a Yule-Nielsen factor [39]. The accuracy of the cellular Yule-Nielsen spectral Neugebauer model (CYNSN) improves in general the accuracy of the plain YNSN model since the physical printer transfer function is sampled on more than the 2^k Neugebauer primaries for a k colorant printer. The main drawback of dealing with this model is the need of more measurements. For that reason it is necessary to find a good compromise between measurement effort and spectral accuracy.

2.13 Kubelka-Munk

The Kubelka-Munk equation defines a relationship between spectral reflectances of the sample and its absorption and scattering characteristics of the samples with opacities greater than 75% using the equation:

$$\frac{K}{S} = \frac{(1 - 0.01R(\lambda))^2}{2(0.01R(\lambda))} \tag{2.9}$$

Where R is the reflectance given in percent and K and S are the absorption and scattering coefficients of the colorant. These ratios are calculated for all colorants separately and then used for computing the K/S ratio of the mixture where those colorants are used. This can be done just by extending the above Kubelka-Munk theory. This is represented as following:

$$\hat{r}(\lambda) = 1 + \frac{K(\lambda)}{S(\lambda)} - [(\frac{K(\lambda)}{S(\lambda)})^2 + 2\frac{K(\lambda)}{S(\lambda)}]^{(\frac{1}{2})} \tag{2.10}$$

Extending the equation further K/S of the mixture is given by the sum of the K/S values of the individual colorants as it follows:

$$\left(\frac{K(\lambda)}{S(\lambda)}\right)_{\text{mixture}} = a\left(\frac{K(\lambda)}{S(\lambda)}\right)_{\text{colorant1}} + b\left(\frac{K(\lambda)}{S(\lambda)}\right)_{\text{colorant2}} + \ldots + \left(\frac{K(\lambda)}{S(\lambda)}\right)_{\text{paper}} \tag{2.11}$$

where a, b, c are the concentrations of the colorants in the mixture.
Finally, value of K/S ratio for all colorants and their combinations is then used in obtaining the reflectances of the primaries and their combinations as follows:

$$R_\infty(\lambda) = 1 + \frac{K(\lambda)}{S(\lambda)} - \sqrt{\left(\frac{K(\lambda)}{S(\lambda)}\right)^2 + 2\frac{K(\lambda)}{S(\lambda)}} \tag{2.12}$$

From the given equations by Kubelka-Munk it can be noticed that this method contains characteristics required in our calculations. Not that is only presented in a very simple mode but it also deals with the scattering problem in the substrate [40]. This consideration is important in our calculations of estimating the Neugebauer Primaries and it will be shown within following chapters.

3 Experimental setup

3.1 Print technologies

In our experimental part two four-channel printers were used for spectral modeling. We had twelve colorant printer channel on dispose(HP Designjet Z3200) but the four-channel ones were still chosen over it. The reason to that was control of the twelve-colorant printer that could not be done with exact precision. For both four channel printers we were able to control all of the channels, cyan, magenta, yellow and black. These two printers are in the same time represents of two different print technologies. Xerox Phaser 6250 use laser print technology while Oce ColorWave600 uses CrystalPoint technology.

3.1.1 Laser print technology

Laser printers rely on the same technology that is used in photocopying machines. This process is known as electrophotography. Electrophotographic process in laser printers, involves six basic steps:

1. A photosensitive surface (photoconductor) is uniformly charged with static electricity by a corona discharge.
2. The charged photoconductor is exposed to an optical image through light to discharge it selectively and forms a latent or invisible image.
3. Development is done by spreading toner, a fine powder, over the surface, which adheres only to the charged areas, thereby making the latent image visible.
4. An electrostatic field transfers the developed image from the photosensitive surface to a sheet of paper.
5. Transferred image is fixed permanently to the paper, by fusing the toner with pressure and heat.
6. Cleaning of all excess toner and electrostatic charges from the photoconductor to make it ready for next cycle.

Laser printers are among the ones that offer the best print quality i.e. the highest resolution. The unique difference is the method of exposition or formation of the latent image. These printers rely on a laser beam and scanner assembly to form a latent image on the photo-conductor bit by bit. The scanning process is similar to electron beam scanning used in CRT. The laser beam modulated by electrical signals from the printer's controller is directed through a collimator lens onto a rotating polygon mirror (scanner), which reflects the laser beam. Then reflected from the scanner laser beam pass through a scanning lens system, which makes a number of corrections to it and scans on the photoconductor [8].

3.1.2 Crystal point print technology

Oce's color toner technology utilizes toner pearls instead of liquid ink. Moreover that ink is a solid TonerPearl, available in CMYK colorants. When the TonerPearl is heated to 300C it becomes a gel. The gel is jetted onto the plain, untreated paper using an Oce-developed inkjet head and dries instantly upon hitting the media. Inkjet technology makes use of tiny ink droplets to facilitate direct printing without the device coming into contact with the printed surface. Because this technology enables non-contact printing, it can be applied to all kinds of media and is now being introduced for use in a wide range of fields ranging from general purpose to industrial. The simple structure that combines the inkjet print head with the scanning mechanism offers the merit of keeping device costs down. In addition, since they require no plates, inkjet printers offer the advantage of major savings in printing set up time compared to conventional printing systems that require a fixed printing block or plate, etc. (e.g. screen printing). Since it dries right away, there is no wicking and no spreading of ink. This way the print obtained is sharped in lines, high readability of fine details, and smooth, even area fills. Further, the solid crystals add a silk shine on plain paper.

3.1.3 Experiment

For our experiment we have used two CMYK printers for spectral modeling, Xerox Phaser 6250 color laser printer and HP 1220C DeskJet printer. Both printers are a 4 channel (CMYK) printers. The colorant combinations have been printed on different types of paper. For laser print staple copy paper $(80g/m^2)$ was used, this was sheet fed printer. In other printer, using crystal point technology for printing, Red Label paper, of gramature $80g/m^2$, was printed on. This was roll though this printer is as well sheet fed printer. For obtaining data used in our spectral printer modeling calculation test chart Linear CMYK i1 i0 P.M. 5.0.7 was used. It is created of all together 128 patches, containing four different color ramps, one per primary channel. Also, one ramp consist of 30 sub-patches or thirty steps gradually increasing to final patch that is full coverage of primary colorant. This test chart was suitable for our work because it has all four channels ramps of the primaries in printers being spectrally modeled. This is represented with figure 9 For

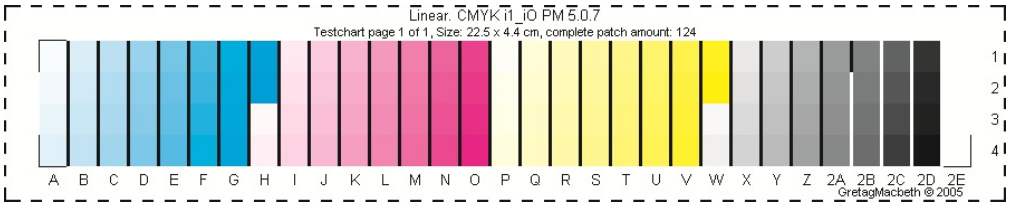

Figure 9: Testchart that is created with linear steps in amount of colorant being placed on paper substrate. This way ramps of printer's primaries were created.

visualizing and printing the chart we used Adobe Photoshop CS5. The main reason to that option was to assure that no color management will be employed while printing process. This was done by testchart opened in CMYK mode and since the testchart is actual TIFF file, we were able to find pure and independent primary prints by setting both monitor and printer color management off. In example, magenta patch of the testchart contains only magenta printer colorant after a

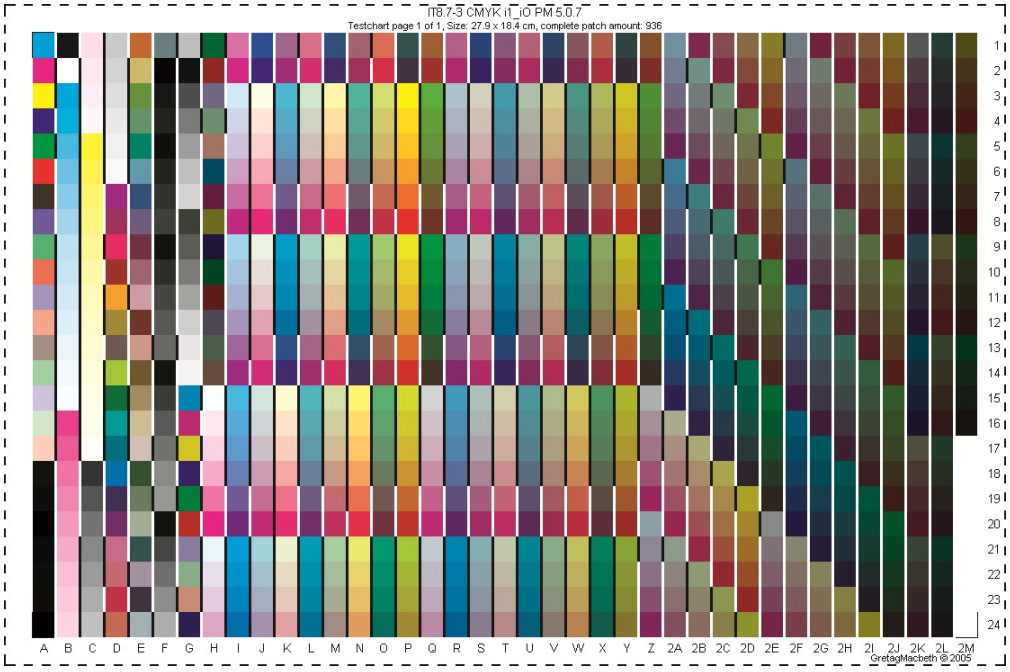

Figure 10: Testchart that is created with four channels and their combinations. This testchart was used for Neugebauer primaries inputs and later as test material in modeling.

print being made. This was the case for both the printers. This way it was possible to be sure that the rest colorants will be printed independent like magenta was. It was important to us to verify this step to make sure that the primaries of our printers are independent of each other and there will not be any unnecessary mixing of colorants in printing ramps of pure channels.

3.2 Instrumentation

Among the spectrophotometers in our laboratory GretagMacbeth Spectrolino was chosen to be used in measuring spectral reflectance of the printed testcharts. Advantage of this instrument is that it can be positioned exactly on color and paper charts for accurate measurements not manually but using software options to control position over the measured sample. To ensure consistent results, Spectrolino uses an annular lens optical system. This multi-directional approach to gathering light in a circle enables Spectrolino to read the target at any angle. It also includes a UV cut filter and has a 45/0 geometry, i.e. with a D50 light source illuminating the printed sample at an angle 45 degrees and a sensor capturing the reflected spectrum at 0 degrees. The UV filter was used for removing effects of optical brightness of the papers. To get the exact spectral reflectance data Spectrolino was combined with measure tool software of Profile Maker pro 5.0.9 for measuring test charts. For measuring Neugebauer primaries another test chart was used, IT8.7-3 CMYK i1-i0 PM 5.0.7. presented with figure 10 That chart is created of total 936 patches, primaries and their combination that also includes Neugebauer primaries. Here the automated work of Spectrolino spectrophotometer was recognized as advantage because it saved

us a lot of time comparing to manually placing the instrument over each patch of test chart.

3.3 Metrics of measured and tested patches

Spectral reflectance measurement of the patches was conducted with self backing process. Testcharts were measured with GretagMacbeth Spectrolino by placing them on the 20 similar blank papers. Spectral reflectance of printed NPs was obtained that way and then and compared with the estimated once. Both spectral and colorimetric distance metrics were employed in obtaining final results [41]. In that way it can be noticed how much diverse they are both spectrally and perceptually. For that reason average root mean square error (RMSE) and goodness of fit coefficient (GFC) between the measurements of spectral reflectances of NPs: measured, estimated and mixed combination and actual measurements of the 108 colorant combination patches of the test chart. These 108 patches were extracted from IT8.7-3 CMYK i1-i0 PM 5.0.7 testchart 10. from field N1 to R12.

The root mean square error (RMSE) for evaluation of spectral estimation was obtain as follows:

$$\mathrm{RMSE} = \left(\frac{1}{n} \sum_{\lambda} (r_m(\lambda) - r_e(\lambda))^2 \right)^{\frac{1}{2}} \tag{3.1}$$

where $r_m(\lambda)$ and $r_e(\lambda)$ are the measured and estimated spectral reflectances. The n value here corresponds to the number of the wavelengths. the perfect match of the $r_m(\lambda)$ and $r_e(\lambda)$ equals to zero nad the worst match goes to infinity.

The Goodness-of-Fit Coefficient (GFC) is the multiple correlation coefficient, the square root of the all $r_e(\lambda)$ estimated spectral variance with the respect to the measured original spectral data of $r_m(\lambda)$ is as follows:

$$\mathrm{GFC} = \frac{\left| \sum_j r_m(\lambda_j) r_e(\lambda_j) \right|}{\left(\sum_j [r_m(\lambda_j)]^2 \right)^{\frac{1}{2}} \left(\sum_j [r_e(\lambda_j)]^2 \right)^{\frac{1}{2}}} \tag{3.2}$$

The GFC is ranged from 0 to 1 and the perfect match equals to 1. GFC value of 0.999 is considered very good spectral match

.

Average ΔEab, $\Delta E94$ and $\Delta E00$ for illuminant D50 were also calculated.
ΔEab

$$\Delta E^*_{ab} = \sqrt{(L^*_2 - L^*_1)^2 + (a^*_2 - a^*_1)^2 + (b^*_2 - b^*_1)^2} \tag{3.3}$$

$\Delta E94$

$$\Delta E^*_{94} = \sqrt{\left(\frac{\Delta L^*}{K_L}\right)^2 + \left(\frac{\Delta C^*_{ab}}{1+K_1 C^*_1}\right)^2 + \left(\frac{\Delta H^*_{ab}}{1+K_2 C^*_1}\right)^2} \tag{3.4}$$

where

$$\Delta L^* = L^*_1 - L^*_2$$
$$C^*_1 = \sqrt{{a^*_1}^2 + {b^*_1}^2}$$
$$C^*_2 = \sqrt{{a^*_2}^2 + {b^*_2}^2}$$
$$\Delta C^*_{ab} = C^*_1 - C^*_2$$
$$\Delta H^*_{ab} = \sqrt{{\Delta E^*_{ab}}^2 - {\Delta L^*}^2 - {\Delta C^*_{ab}}^2} = \sqrt{{\Delta a^*}^2 + {\Delta b^*}^2 - {\Delta C^*_{ab}}^2}$$
$$\Delta a^* = a^*_1 - a^*_2$$
$$\Delta b^* = b^*_1 - b^*_2$$

ΔE00

$$\Delta E^*_{00} = \sqrt{\left(\frac{\Delta L'}{S_L}\right)^2 + \left(\frac{\Delta C'}{S_C}\right)^2 + \left(\frac{\Delta H'}{S_H}\right)^2 + R_T \frac{\Delta C'}{S_C}\frac{\Delta H'}{S_H}} \tag{3.5}$$

where

$$\Delta L' = L^*_2 - L^*_1$$

$$\bar{L} = \frac{L^*_1 + L^*_2}{2} \quad \bar{C} = \frac{C^*_1 + C^*_2}{2}$$

$$a'_1 = a_1 + \frac{a_1}{2}\left(1 - \sqrt{\frac{\bar{C}^7}{\bar{C}^7 + 25^7}}\right) \quad a'_2 = a_2 + \frac{a_2}{2}\left(1 - \sqrt{\frac{\bar{C}^7}{\bar{C}^7 + 25^7}}\right)$$

$$\bar{C}' = \frac{C'_1 + C'_2}{2} \text{ and } \Delta C' = C'_2 - C'_1 \quad \text{where } C'_1 = \sqrt{a_1'^2 + b_1^2} \quad C'_2 = \sqrt{a_2'^2 + b_2^2}$$

$$h'_1 = \tan^{-1}(b_1/a'_1) \mod 2\pi, \quad h'_2 = \tan^{-1}(b_2/a'_2) \mod 2\pi$$

$$\Delta h' = \begin{cases} h'_2 - h'_1 & |h'_1 - h'_2| \le \pi \\ h'_2 - h'_1 + 2\pi & |h'_1 - h'_2| > \pi, h'_2 \le h'_1 \\ h'_2 - h'_1 - 2\pi & |h'_1 - h'_2| > \pi, h'_2 > h'_1 \end{cases}$$

$$\Delta H' = 2\sqrt{C'_1 C'_2}\sin(\Delta h'/2), \quad \bar{H}' = \begin{cases} (h'_1 + h'_2 + 2\pi)/2 & |h'_1 - h'_2| > \pi \\ (h'_1 + h'_2)/2 & |h'_1 - h'_2| \le \pi \end{cases}$$

$$T = 1 - 0.17\cos(\bar{H}' - \pi/6) + 0.24\cos(2\bar{H}') + 0.32\cos(3\bar{H}' + \pi/30) - 0.20\cos(4\bar{H}' - 21\pi/60)$$

$$S_L = 1 + \frac{0.015\left(\bar{L} - 50\right)^2}{\sqrt{20 + \left(\bar{L} - 50\right)^2}} \quad S_C = 1 + 0.045\bar{C}' \quad S_H = 1 + 0.015\bar{C}'T$$

$$R_T = -2\sqrt{\frac{\bar{C}'^7}{\bar{C}'^7 + 25^7}} \sin\left[\frac{\pi}{6}\exp\left(-\left[\frac{\bar{H}' - 275^\circ}{25}\right]^2\right)\right]$$

3.4 Estimation of Neugebauer Primaries

After measuring exact spectral reflectance data of Neugebauer primaries from the test charts estimation of the same patches being measured was done. In our experiment estimation of the NPs reflectances was obtained by using Kubelka-Munk theory mentioned previously explained in 2.13. Measured reflectances of the primary colorants of the printers were used as a starting point for the estimation of the reflectance of the rest of the NPs. First, we calculate the K/S ratios for these primaries. Then we used these ratios in order to compute the K/S ratios for the combinations of CMYK primaries. In the end, the reflectance of each NPs from their resulted K/S ratios was computed. The 16 NPs were printed by both printers from IT8.7-3 CMYK i1-i0 PM 5.0.7 testchart, both on different paper substrate.

3.5 Spectral modeling of the Oce ColorWave600 printer

The process of modeling the CrystalPoint technology printer Oce ColorWave600 started with the measuring the color patches from the Linear testchart 10 where the ramps were given for all the four channels of printer. The spectral reflectances of measured ramps are given with fig. 11 for cyan, fig. 12 for magenta, fig. 13 and fig. 14 for yellow and black.

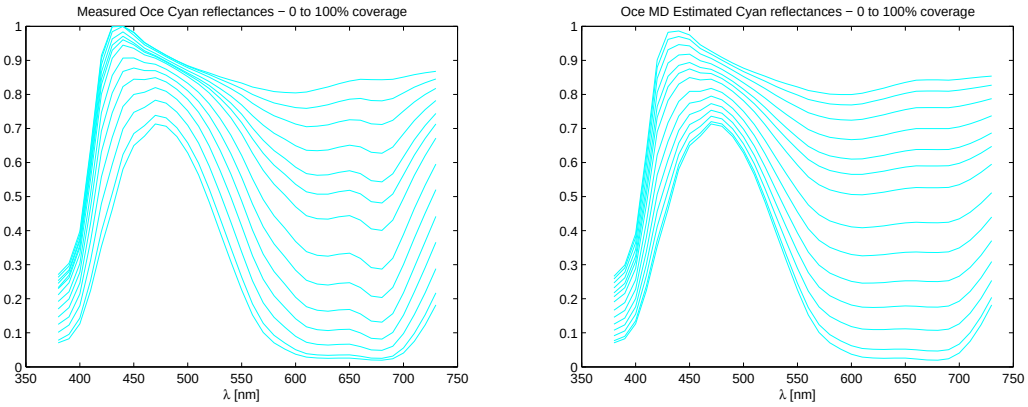

Figure 11: Oce - measured and estimated spectral reflectances of cyan ramp.

After the Linear testchart was printed the theoretical coverage values were replaced with the effective coverage values by inverting the Murray-Davies spectral print model. The obtained effective colorant values confirms the dot gain effect. This can be seen from the fig. 15

Once when the colorant coverage was established from actual printed values the estimation of the color ramps was started. This needed to be conducted for each of the ramp of the linear

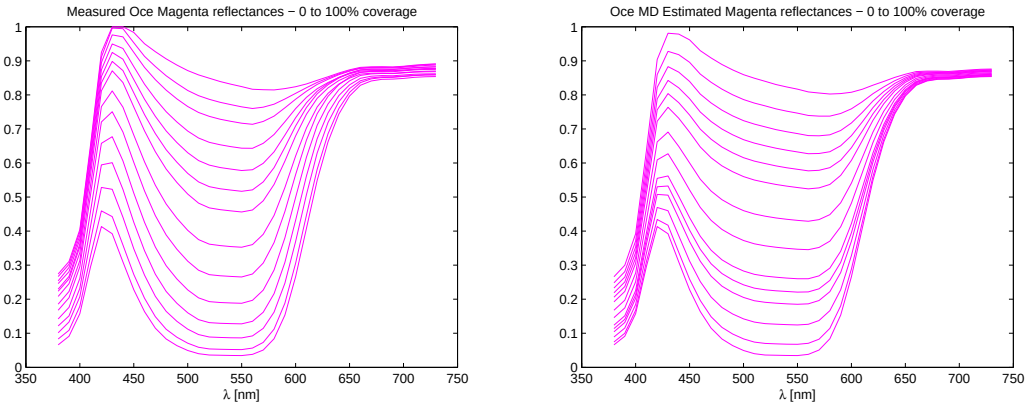

Figure 12: Oce - measured and estimated spectral reflectances of magenta ramp.

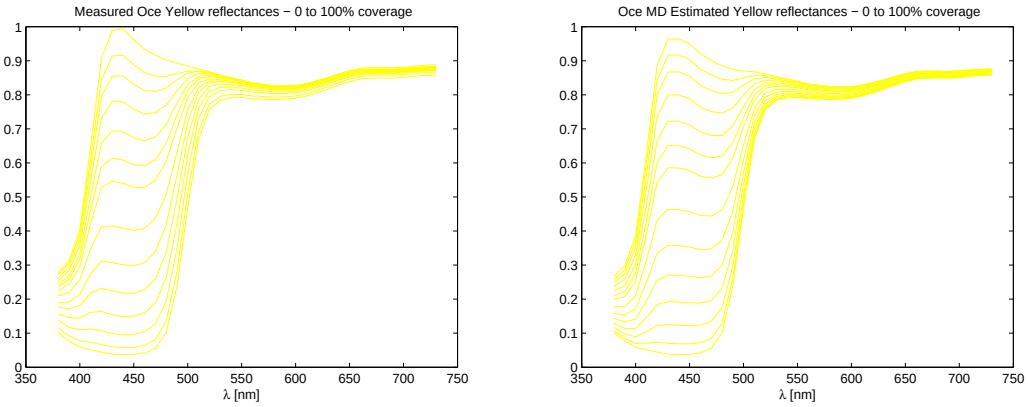

Figure 13: Oce - measured and estimated spectral reflectances of yellow ramp.

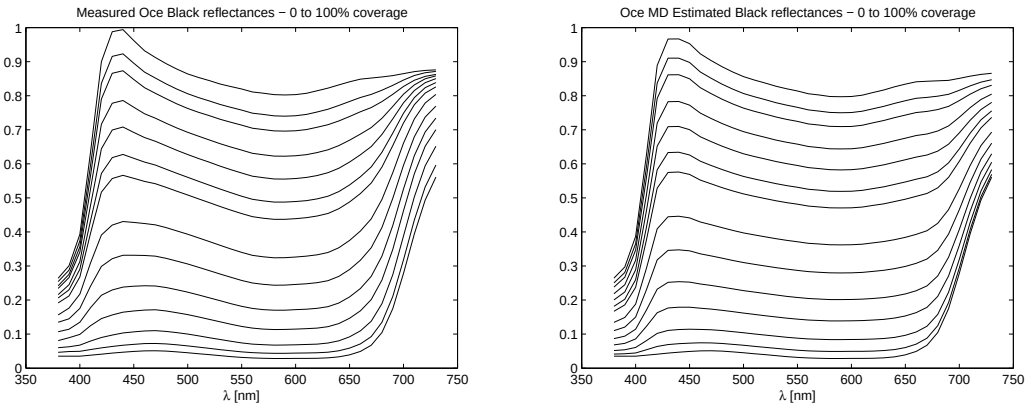

Figure 14: Oce - measured and estimated spectral reflectances of black ramp.

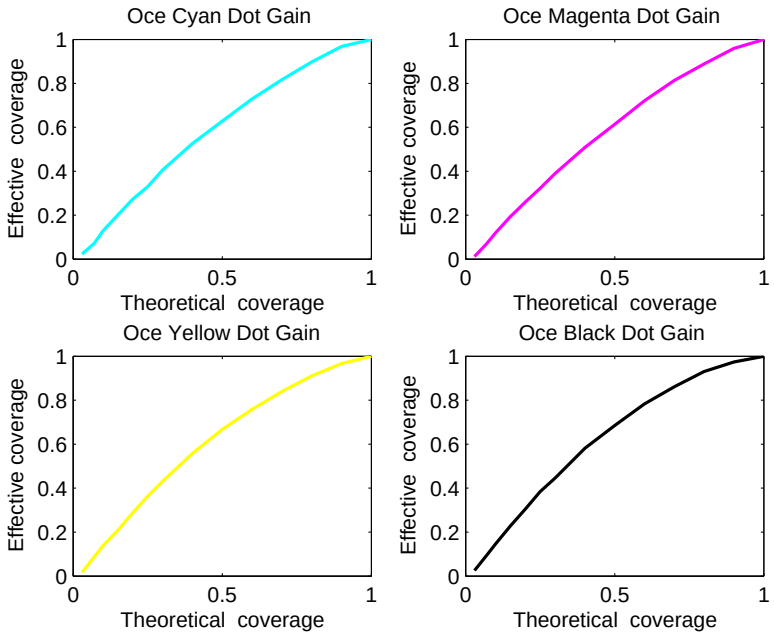

Figure 15: Effective colorant coverage of Oce ColorWave 600 printer.

testchart separately since the effective coverage is specific for the each colorant channel. The fact that the ramps were monochromatic resulted with using Murray-Davies model in process of estimation. Predicted spectral reflectances are shown in fig. 11 for cyan, fig. 12 for magenta, fig. 13 and fig. 14 for yellow and black ramp. It can be seen that the estimated reflectances are more uniform comparing to measured spectral reflectances. In case when the effective coverage was not considered the uniformity of the spectral reflectances curve is even more expressed. This is due to dot gain effect and not considering variables as effective coverage or later on, the n value.

3.6 Xerox printer

The process of modeling the laser technology printer Xerox Phaser 6250 started with the measuring the color patches from the Linear testchart 10 where the ramps were given for all the four channels of printer. The spectral reflectances of measured ramps are given with fig. 16 for cyan, fig. 17 for magenta, fig. 18 and fig. 19 for yellow and black.

After the Linear testchart was printed the theoretical coverage values were replaced with the effective coverage values with inverting the Murray-Davies spectral print model. The obtained effective colorant values confirms the dot gain effect. This can be seen in fig. 20.

The modeling process was the same in steps as it was for the Oce ColorWave600 printer. Once when the colorant coverage was established from actual printed values the estimation of the color ramps was started. This needed to be conducted for each of the ramp of the linear testchart separately since the effective coverage is specific for the each colorant channel. The

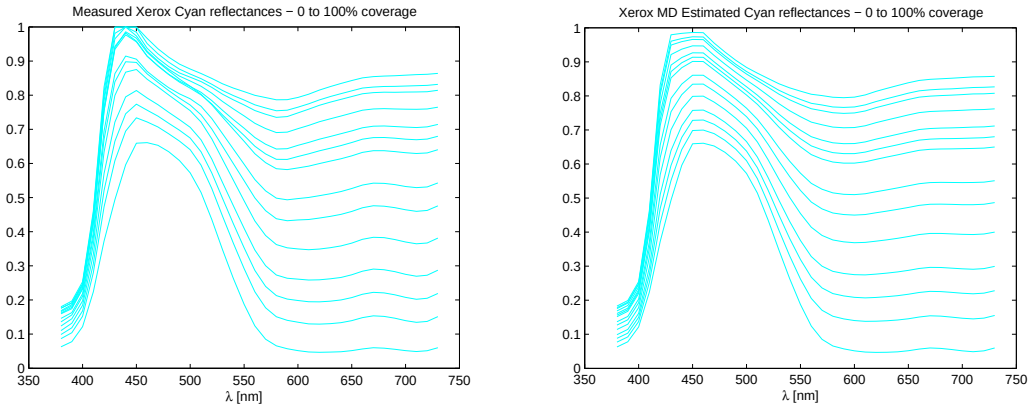

Figure 16: Xerox - measured and estimated spectral reflectances of cyan ramp.

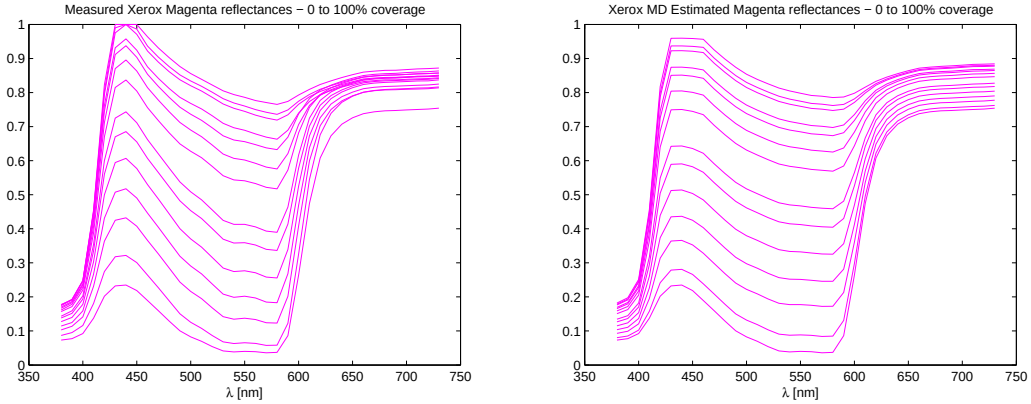

Figure 17: Xerox - measured and estimated spectral reflectances of magenta ramp.

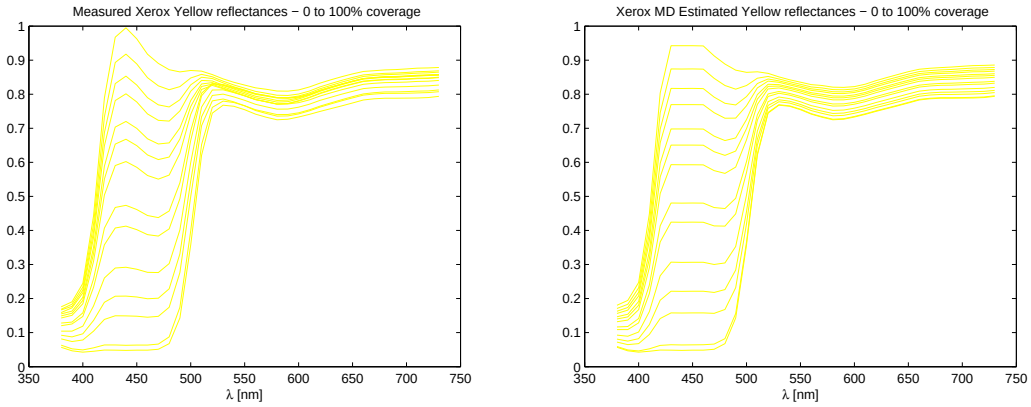

Figure 18: Xerox - measured and estimated spectral reflectances of yellow ramp.

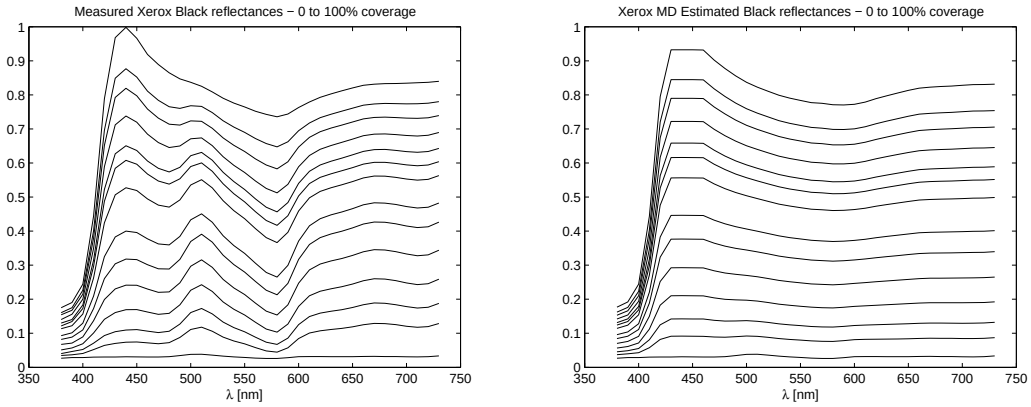

Figure 19: Xerox - measured and estimated spectral reflectances of black ramp.

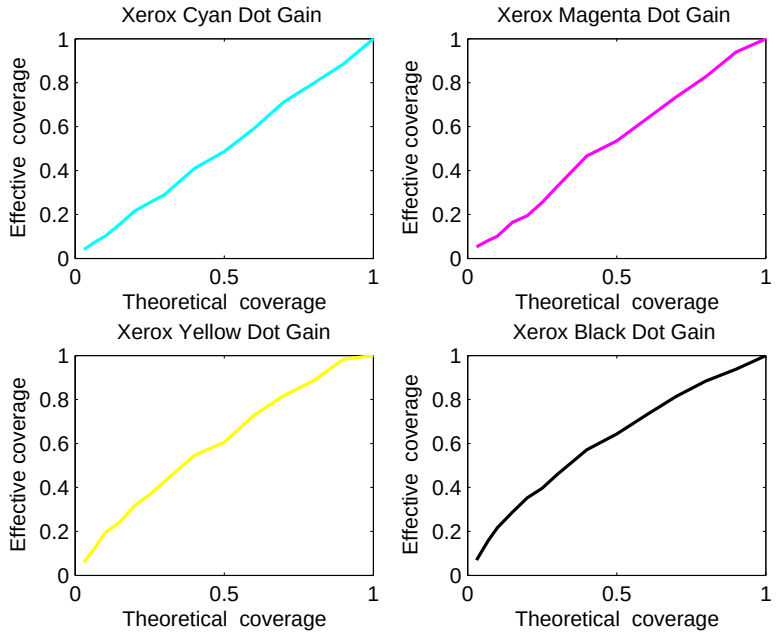

Figure 20: Effective colorant coverage of Xerox Phaser 6250 printer.

fact that the ramps were monochromatic resulted with using Murray-Davies model in process of estimation. Predicted spectral reflectances are shown in fig. 16 for cyan, fig. 17 for magenta, fig. 18 and fig. 19 for yellow and black ramp. It can be seen that the estimated reflectances are more uniform comparing to measured spectral reflectances. In case when the effective coverage was not considered the uniformity of the spectral reflectances curve is even more expressed because of neglecting the effect of the dot gain effect and not considering the n value. That will be further done with YNSN model.

4 Spectral printer modeling - results

4.1 Kubelka-Munk theory

In the process of estimating reflectances the Kubelka-Munk equation was employed:

$$\hat{r}(\lambda) = 1 + \frac{K(\lambda)}{S(\lambda)} - [(\frac{K(\lambda)}{S(\lambda)})^{2} + 2\frac{K(\lambda)}{S(\lambda)}]^{(\frac{1}{2})} \tag{4.1}$$

$$\left(\frac{K(\lambda)}{S(\lambda)}\right)_{\text{mixture}} = a\left(\frac{K(\lambda)}{S(\lambda)}\right)_{\text{colorant1}} + b\left(\frac{K(\lambda)}{S(\lambda)}\right)_{\text{colorant2}} + \ldots + \left(\frac{K(\lambda)}{S(\lambda)}\right)_{\text{paper}}$$

$$R_{\infty}(\lambda) = 1 + \frac{K(\lambda)}{S(\lambda)} - \sqrt{\left(\frac{K(\lambda)}{S(\lambda)}\right)^{2} + 2\frac{K(\lambda)}{S(\lambda)}}$$

This way the relationship between spectral reflectances of the patch and its absorption and scattering characteristics of the patch were established [42] [43]. This was very useful because ratio K/S of the mixture is given by the sum of the K/S values of the individual colorants which are primaries of printer [44] [45]. Finally, K/S ratio for all of primaries colorants and their combinations is then used in obtaining the estimated reflectances of the primaries and their combinations respectively. This is shown in figure 21 for the Oce ColorWave 600 printer and then with figure 22 for the Xerox Phaser 6250.

4.2 Spectral Neugebauer model

Testing this model was important step because it considers all the channels of a printer and by extending initial Murray-Davies model [46]. This way we were able to calculate spectral reflectance value of possible combinations of colorants by taking into account 100% (full) colorant coverage of primaries. By using equation 2.5 tested patches the following results were obtained in 23 and 24.

Comparing the results obtained for the modeling of both printers with the Spectral Neugebauer model lead to several conclusions to be read from the tables presented. If comparing technologies for this particular model the laser technology resulted with more accurate values. Futher, moving to measured, estimated and mixed combination of the Neugebauer primaries tested on 108 extracted patches from testchart resulted with the best calculations for the mixed combination. That value was obtained with the $\Delta E00$.

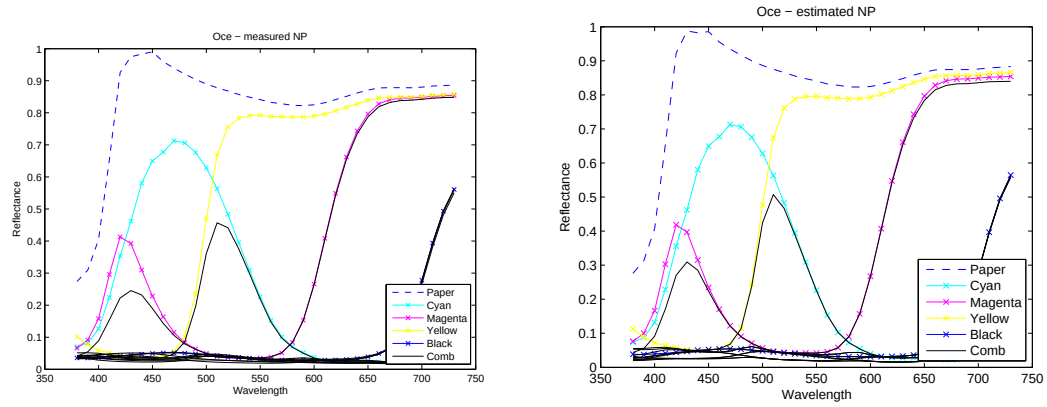

Figure 21: Visualization of measured Neugebauer primaries and Neugebauer primaries estimated using Kubelka Munk equation for Oce ColorWave 600 printer.

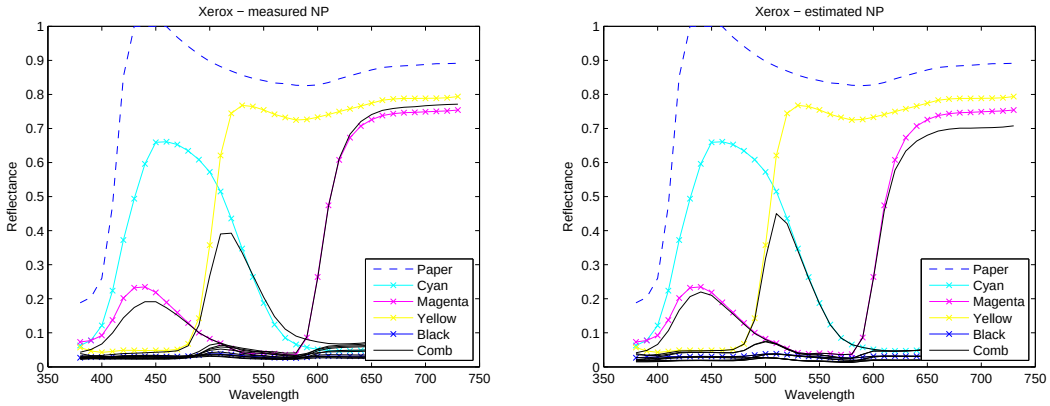

Figure 22: Visualization of measured Neugebauer primaries and Neugebauer primaries estimated using Kubelka Munk equation for Xerox Phaser 6250 printer.

	SN - Océ ColorWave 600								
NPs	mNPs			eNPs			mixNPs		
	mean	max	std	mean	max	std	mean	max	std
sRMSE	0,059	0,061	0,019	0,062	0,069	0,007	0,061	0,072	0,009
GFC	0,993	0,974	0,008	0,992	0,987	0,004	0,994	0,985	0,005
ΔE	7,98	20,41	2,47	7,82	12,45	2,84	7,02	13,24	2,14
ΔE94	5,8	15,41	2,72	6,2	14,57	3,01	5,96	13,24	3,45
ΔE00	5,2	13,21	1,95	5,97	14,87	2,32	5,48	9,97	2,41

Figure 23: Results of Spectral Neugebauer model for Oce ColorWave 600 printer.

	SN - Xerox Phaser 6250								
NPs	mNPs			eNPs			mixNPs		
	mean	max	std	mean	max	std	mean	max	std
sRMSE	0,045	0,051	0,021	0,043	0,132	0,019	0,041	0,112	0,012
GFC	0,996	0,972	0,003	0,995	0,919	0,008	0,996	0,909	0,009
ΔE	7,02	19,01	4,01	7,3	20,47	4,02	6,99	15,45	5,14
ΔE94	5,39	16,21	2,54	5,84	12,47	2,41	5,58	2,24	3,21
ΔE00	5,04	14,95	2,75	5,5	16,81	2,13	5,02	2,04	2,45

Figure 24: Results of Spectral Neugebauer model for Xerox Phaser 6250 printer.

4.3 Yule-Nielsen Modified Spectral Neugebauer Model

With this model the nonlinear relationship between the reflection spectra of paper and colorant placed was tested. This was done by applying a power function, whose exponent n is fitted according to a limited set of measured patch reflection spectra. With the non-linear relationship being applied the results obtained were more accurate than the ones obtained with spectral Neugebauer model. That can be read, for both of the printers, from 25 and 26

	YNSN - Océ ColorWave 600											
NPs	mNPs				eNPs				mixNPs			
	n	mean	max	std	*n*	mean	max	std	*n*	mean	max	std
sRMSE	3,5	0,042	0,049	0,005	3,5	0,047	0,051	0,005	4,3	0,055	0,068	0,004
GFC	4,2	0,994	0,991	0,009	4,5	0,994	0,991	0,002	4,2	0,997	0,984	0,005
ΔE	1,9	7,1	15,32	2,31	2,1	7,5	10,21	1,95	1,9	6,95	11,54	1,95
ΔE94	2,1	5,2	16,14	3,12	2,2	5,96	12,41	2,31	2,1	4,97	10,24	3,2
ΔE00	2,4	4,64	12,98	3,1	2,4	5,02	12,23	2,41	2,7	5,02	8,41	2,1

Figure 25: Results of Yule-Nielsen Modified Spectral Neugebauer model for Oce ColorWave 600 printer.

	YNSN - Xerox Phaser 6250											
NPs	mNPs				eNPs				mixNPs			
	n	mean	max	std	*n*	mean	max	std	*n*	mean	max	std
sRMSE	3,3	0,036	0,039	0,009	3,3	0,039	0,091	0,009	3,3	0,049	0,102	0,004
GFC	4,1	0,997	0,978	0,01	3,9	0,995	0,923	0,004	4,6	0,996	0,959	0,007
ΔE	2,3	6,2	11,45	2,14	2,3	6,9	15,41	2,31	2,3	7,1	14,21	3,89
ΔE94	2,3	4,5	10,12	2,01	2,3	4,8	10,21	3,1	2,7	5,21	10,25	2,14
ΔE00	2,0	4,2	9,21	1,95	2,1	4,51	14,32	2,03	2,6	4,91	9,87	1,54

Figure 26: Results of Yule-Nielsen Modified Spectral Neugebauer model for Xerox Phaser 6250 printer.

The calculations obtained for the modeling of both printers with the Yule-Nielsen Modified Spectral Neugebauer Model resulted with conclusions to be read from the tables presented. When

comparing technologies for this particular model the laser technology again resulted with more accurate values. Comparing measured, estimated and mixed combination of the Neugebauer primaries tested on 108 extracted patches from testchart resulted with the best calculations for the patches not being estimated or mixed but measured. That value was obtained with the ΔE00. Introducing optimal n value in this model has shown results being noticeable improved. This is because now not only mechanical but the optical dot gain was considered.

4.4 Cellular spectral Neugebauer Model

With testing cellular spectral Neugebauer model the goal was to reduce the space over which interpolation is performed. This was done by providing more primaries by measuring each colorant at 0, 50, and 100% area coverage. This also means that the printer gamut is subdivided into smaller cells comparing to binary system of placing colorant (placed: 100% or not placed:0%) on substrate. By applying all these constrains the following results were obtained for Oce ColorWave 600 27 and Xerox Phaser 6250 28 In case of the calculations obtained for the modeling of both

	cSN - Océ ColorWave 600								
NPs	mNPs			eNPs			mixNPs		
	mean	max	std	mean	max	std	mean	max	std
sRMSE	0,04	0,049	0,018	0,041	0,062	0,009	0,042	0,059	0,012
GFC	0,997	0,98	0,005	0,997	0,967	0,012	0,998	0,98	0,004
ΔE	6,5	10,45	1,95	6,8	12,45	2,14	6,52	13,54	2,45
ΔE94	5,1	12,45	2,14	5,45	13,21	1,92	5,12	12,14	4,21
ΔE00	4,1	10,27	2,12	4,9	13,71	2,52	4,15	11,25	2,41

Figure 27: Results of Cellular spectral Neugebauer model for Oce ColorWave 600 printer.

	cSN - Xerox Phaser 6250								
NPs	mNPs			eNPs			mixNPs		
	mean	max	std	mean	max	std	mean	max	std
sRMSE	0,03	0,041	0,004	0,032	0,049	0,011	0,03	0,051	0,012
GFC	0,997	0,991	0,004	0,997	0,991	0,002	0,998	0,987	0,004
ΔE	5,98	13,21	2,45	6,12	12,54	2,51	6,1	15,12	2,98
ΔE94	4,15	13,25	2,02	4,2	11,49	1,97	4,5	14,21	3,14
ΔE00	3,95	11,47	1,98	4,1	12,03	1,48	4,23	15,21	3,87

Figure 28: Results of Cellular spectral Neugebauer model for Xerox Phaser 6250 printer.

printers with the Cellular spectral Neugebauer Model resulted with conclusions to be read from

the tables presented. When comparing technologies for this particular model the laser technology again resulted with more accurate values. Comparing measured, estimated and mixed combination of the Neugebauer primaries tested on 108 extracted patches from testchart resulted with the best calculations for the patches that were measured have shown the best result.Nevertheless, values very close to that are the ones obtained with mix both measured and estimated vales of Neugebuer Primaries. That most accurate value was obtained with the ΔE00. Introducing the smaller cell (range 0,0.5,1 instead only 0 to 1) in this model has shown results being significantly improved. This is due to decreasing the size of the cell that enables interpolation to be more precise.

4.5 Cellular Yule-Nielsen spectral Neugebauer model

When the testing of cellular spectral Neugebauer model was extended with addition of a Yule-Nielsen factor the accuracy was shown to be improved. The reason was that with this model(cYNSN), unlike with plain YNSN model, physical printer transfer function is sampled on more than the 2^k Neugebauer primaries for a k colorant printer. That was the 50% coloranat coverage added that made cell smaller, therefore more accurate. The results can be read from 29 for Oce ColorWave 600 and 30 for Xerox Phaser 6250 printer. The calculations obtained for the modeling of both

	cYNSN - Océ ColorWave 600											
NPs	mNPs				eNPs				mixNPs			
	n	mean	max	std	*n*	mean	max	std	*n*	mean	max	std
sRMSE	3,1	0,031	0,04	0,009	3,4	0,035	0,039	0,004	3,5	0,035	0,045	0,009
GFC	3,9	0,997	0,988	0,007	4,2	0,997	0,995	0,002	4,1	0,998	0,991	0,006
ΔE	1,5	5,45	14,31	2,2	1,6	5,9	9,52	2,12	1,9	6,15	10,25	2,35
ΔE94	1,8	3,82	12,38	3,4	2,1	5,1	9,89	2,98	2,1	4,25	10,89	3,98
ΔE00	2,1	3,5	10,6	2,9	2,4	3,8	10,25	2,54	2,3	4,83	9,45	3,25

Figure 29: Results of Cellular Yule-Nielsen spectral Neugebauer model for Oce ColorWave 600 printer.

	cYNSN - Xerox Phaser 6250											
NPs	mNPs				eNPs				mixNPs			
	n	mean	max	std	*n*	mean	max	std	*n*	mean	max	std
sRMSE	3,3	0,028	0,031	0,008	3,2	0,032	0,038	0,007	4,5	0,035	0,055	0,004
GFC	4,1	0,998	0,989	0,009	4,1	0,997	0,988	0,007	5,2	0,997	0,987	0,006
ΔE	2,3	5,15	12,35	3,45	2,4	6,12	14,58	3,65	2,3	6,52	13,24	3,47
ΔE94	2,3	3,98	10,78	2,45	2,9	4,2	11,24	2,54	2,3	4,52	9,66	2,1
ΔE00	2,0	3,2	8,52	2,86	2,7	4,1	13,22	2,02	2,0	4,98	8,41	2,33

Figure 30: Results of Cellular Yule-Nielsen spectral Neugebauer model for Xerox Phaser 6250 printer.

printers with the Cellular Yule-Nielsen spectral Neugebauer model resulted with conclusions to be read from the tables presented. When comparing technologies for this particular model the laser technology does not show more accurate values comparing to Oce printer at it was previous case. When used measured spectral reflectances of the Neugebauer primaries Xerox does

give the higher accuracy values obtained. Neverthless, in estimated and mixed Neugebeuer primaries Oce printer results with more accurate values. this is in case of calculation obtained with the $\Delta E00$. Introducing optimal n value and making the cell smaller (range 0,0.5,1 instead only 0 to 1) in this model has shown results being significantly improved as well as having optimal $n$values considered. This is result of to decreasing the size of the cell that enables interpolation to be more precise, as well as taking into account not only mechanical but the optical dot gain effect.

5 Feasibility of spectral print reproduction

In previous chapters spectral printer modeling was explained. Spectral printer models were also performed for two printers of different printing technology. The results were different for laser technology comparing to crystal point which is extension of inkjet technology. Both of the printers were using four channels for spectral print reproduction. This fact put in front of us interesting question: will increasing the number of colorant channels also increase possibility to reach the exact spectral color reproduction. In order to answer this question fundamental knowledge of halftoning process should be considered [47] [48] [49]. That process can be started by placing two colorants on paper substrate and then comparing the obtained complete subset of colors with the same result of placing four colorants. From that example it is possible to observe that color gamut, which is obtained with complete subset of colors printed, plays very important role in making any further conclusion. The subset of colors which can be accurately represented in a given circumstance, such as within a given color space or by a certain output device.The process of printing any combinations of colorants nowadays is set to high accuracy that is followed by high level reproduction. This is due to fast development of new technologies that enable better control of the printer and printing system [50]. Starting with the spectral color reproduction input instruments give high precision of data collected but the challenge is still in creating the precise communication between the input measurements and wanted printed material. Starting from the point where the issues of creating the output product are well known the importance of assuring the spectral print of that product is possible at all becomes more significant and valuable information. The reason is the waste of resources, colorants and paper as well as time. It is important to have confirmation that the spectral reflectances wanted to be reproduced are possible with the given characteristic of printer available. For this reason in this part of thesis work the process of deciding weather the spectral print reproduction is possible or not was tried to be automated. The algorithm consisted of few steps that lead to final yes or no was proposed. Having the strong twelve colorant printer on disposition, as well as matching set of different paper substrates available, made this process to give results from which in the end the valuable conclusion on feasibility was made.

5.1 Collaboration with retailer

In this part of thesis focus was on feasibility of particular product. The collaboration with retail store resulted in obtaining the real samples and testing the possibility of spectral print reproduction with printer in our lab. The challenge was in trying to reduce the cost that retailer currently incur on one front of the retail color development process. That particularly involves recurring expenditure on 5 cm x 5 cm fabric samples that are produced to within 0.8 DE CMC. This is valid for illuminant UL3000 and 10 degrees observer. Designers use these physical representations when they are deciding which shade an item of garment product will be, or which shade needs to be placed near another in a printed or yarn dyed pattern on a garment product. The existing

set of roughly 4000 colors is supporting the design process within the color set that designers are able to pick from. Once their colors for a season and brand are picked, 5cm x 5cm fabric samples are ordered to work with. The 4000 colors are supported using spectral data. That reference helps keep the color on shade through many production runs, i.e. of color chips, of the color standards, and of the garments that are specified to be in close tolerance of these colors. With that given one set of spectral data for all colors, within scope of these thesis feasibility of printing particular colors out on as needed basis was tested. The possibility of printing these color samples versus purchasing them from a dyeing company would significantly save in cost per color. That is why the important step was focus on investigation the feasibility of being able to produce these colors accurately and consistently over the many variables that arise during consecutive runs. The starting issue in getting the print head create the wanted output, was to replace the D50 table with a UL3000 illuminant. The reason for that was the fact that color standards are made using reactive dyes, and the printers are limited to a significantly smaller set of colorants. Therefore, from a reflectance curve matching standpoint it was expected that there will likely be gaps. To overcome that problem the try to match to UL3000 illuminant was very important. Another challenge that was related to gamut is the difference in available chroma in the chromophores. Given that there are spectral data for all 4000 colors available, the brightest colors to be produced to produce are known as well but only the right combination of paper and colorants will create the maximum chroma. This is due to having the spectral data for the targets it would be easy to generate the L*,a*,b*, C, and h values for all colors. From this step then it is possible to determine the maximum chroma needed. This would be a base ground for possible realization of coverage for given gamut [51] [52].

5.2 Color Gamut

In color theory, the gamut of a device or process is that portion of the color space that can be represented, or reproduced. Generally, the color gamut is specified in the hue-saturation plane, as a system can usually produce colors over a wide intensity range within its color gamut. For a subtractive color system, as used in printing, the range of intensity available in the system is for the most part meaningless without considering system-specific properties. That property is the illumination of the colorant being placed on paper [53] [54] [55]. In cases when certain colors cannot be expressed within a particular color model, those colors are said to be out of gamut. For example, while pure red can be expressed in the RGB color space, it cannot be expressed in the CMYK color space; pure red is out of gamut in the CMYK color space. Even though modern techniques allow increasingly good approximations, at this moment device that is able to reproduce the entire visible color space is still an unrealized goal within the engineering of printing processes. In processing a digital image the RGB color space is the most convenient color model used. Printing the image requires transforming the image from the original RGB color space to the printer's CMYK color space. During this process, the colors from the RGB which are out of gamut must be converted to approximate values within the CMYK space gamut. Simply trimming only the colors which are out of gamut to the closest colors in the destination space would burn the image. There are several algorithms approximating this transformation, but none of them is perfect. The reason of that is that those colors are simply out of the target device's capabilities.

This is why identifying the colors in an image which are out of gamut in the target color space as soon as possible during processing is critical for the quality of the final print reproduction product.

5.3 Problem specification

What was done by now was the reproduction of the same set of 4000 colors using pigments in an injection molded process. Within that the knowledge that reflectance of colors made while using reactive dyes helped in match and use reflectance curves of pigments. That was why the whole process wanted to be moved to one step further - ink and paper combination. The samples used for our calculation were subset of original set consisted of 4000 samples. The subset consisted of 32 data samples(details in Appendix). Spectral data of a textile standard and a plastic standard for the 10 degree observer weighted illuminant were given. The colors made by injection molding were used as color standards which suppliers in the hard goods area need to match. The idea was to have 'pre-translated' the color difference between textile dyes used in Apparel and Soft home products, and pigments used in Hard home areas.The main goal was to have the L*a*b* values of printed samples to match the L*a*b* values of the standard or have the color difference in terms of CMC DE in UL3000, which is store light, for 10 degree observer between the two be as low as possible. An acceptable difference limit was defined with value of is 0.8 DE CMC. Those that fall outside of that difference up to 1.2 can be given special consideration by using visual determination of color difference. Those above 1.2 can be identified as out of gamut for the system under investigation. Spectral reflection data was obtained on spectrophotometer Datacolor SF600 Plus CT for each associated color. The values of reflectance were measured by this instrument at 10 nm interval starting at 400nm. Datacolor SF600 plus CT has an integrating sphere for illumination of the sample and the detector for the spectral analyzer is placed at 8 degrees from normal to the surface of the aperture plane (sample port). Sample ports are configurable depending on size of sample being presented. LAV (Large Area View) aperture plate is 30 mm illuminated and 26nm measured. This is important for ability to maximize the surface area to be measured which is ideal to measure color without regard to a textured surface.The instrument is dual-beam spectrophotometer with diffuse illumination and high black trap performance [56] [44].

The metric that defines a difference measure used here is CMC. It was created in 1984. by the Colour Measurement Committee of the Society of Dyers and Colourists [57]. It is based on the L*C*h color model. Named after the developing committee, their metric is called CMC l:c. It has two parameters: lightness (l) and chroma (c), allowing the users to weight the difference based on the ratio of l:c that is deemed appropriate for the application. Commonly-used values are 2:1 for acceptability and 1:1 for the threshold of imperceptibility. It is defined with the equations 5.1, 5.2 and 5.2. The distance of a color (L_2^*, C_2^*, h_2) to a reference (L_1^*, C_1^*, h_1) is as follows:

$$\Delta E^*_{CMC} = \sqrt{\left(\frac{L_2^* - L_1^*}{lS_L}\right)^2 + \left(\frac{C_2^* - C_1^*}{cS_C}\right)^2 + \left(\frac{\Delta H^*_{ab}}{S_H}\right)^2} \tag{5.1}$$

where

$$S_L = \begin{cases} 0.511 & L_1^* < 16 \\ \frac{0.040975L_1^*}{1+0.01765L_1^*} & L_1^* \geq 16 \end{cases} \quad S_C = \frac{0.0638C_1^*}{1+0.0131C_1^*} + 0.638 \quad S_H = S_C(FT + 1 - F) \tag{5.2}$$

and where

$$F = \sqrt{\frac{C_1^{*4}}{C_1^{*4} + 1900}} \quad T = \begin{cases} 0.56 + |0.2\cos(h_1 + 168°)| & 164° \leq h_1 \leq 345° \\ 0.36 + |0.4\cos(h_1 + 35°)| & \text{otherwise} \end{cases} \tag{5.3}$$

Figure 31: Datacolor SF600 spectrophotometer.

Figure 32: Lab values of retailer's color samples.

5.4 ICC3D

With given constraints of the error allowed within delta CMC value 0.8 the process of spectral color reproduction was decided to be started with checking the feasibility. Two printers that were used for spectral print modeling were considered to be employed, Xerox Phaser 6250 color laser and Oce ColorWave 600 printer. The process was started with numerical and visual representation of their gamuts. This was done by using color ramps of separated printed colorants. Next, spectral reflection data of ramp was measured with and finally represented with the L*a*b* values by means ICC3D software. The functionality of the ICC3D software is the ability to read color data as an image in some standard format or that are extracted by the gamut tag of an ICC profile. It also enables the color data to be displayed in different ways in various 3D color spaces [58]. This is very useful for visualizing the whole process of checking the spectral print feasibility. The L*a*b* values of the four channels printer and their gamuts are shown with fig. 33 for Xerox Phaser 6250 and fig. 33 for the Oce ColorWave 600 printer.

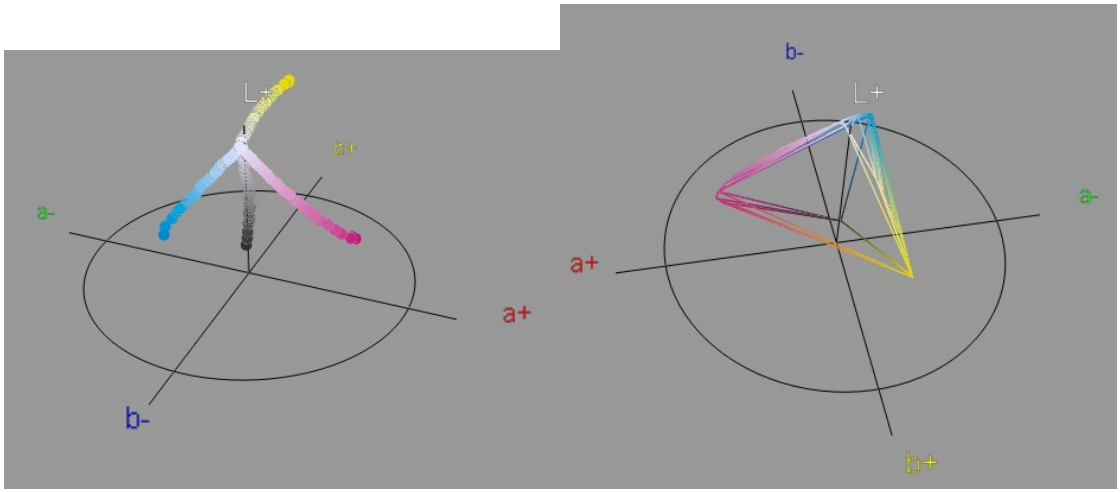

Figure 33: 3D gamut visualization of Xerox Phaser 6250 printer is shown on the right side. On the left side L*a*b* values of ramp printed separately for all four channels is presented.

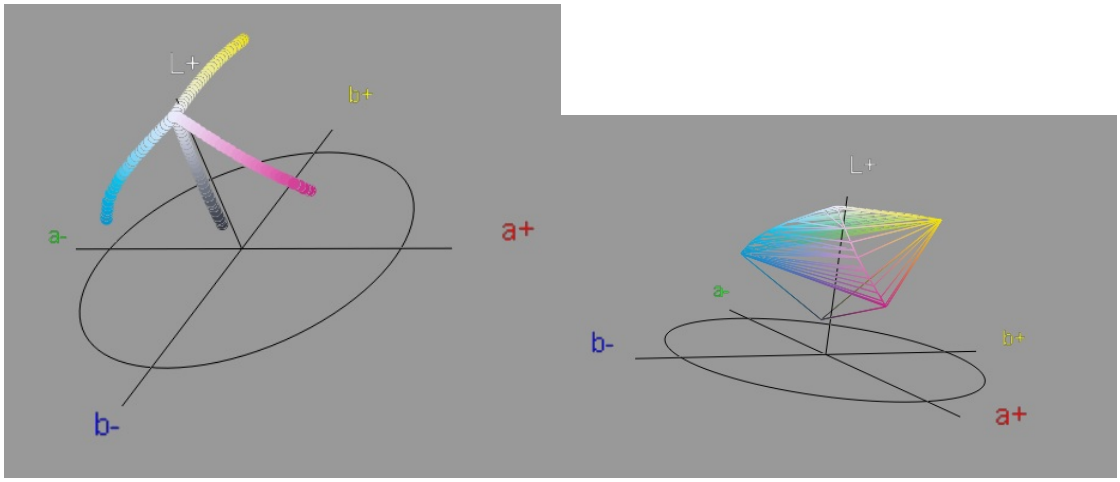

Figure 34: 3D gamut visualization of Oce ColorWave 600 printer is shown on the right side. On the left side L*a*b* values of ramp printed separately for all four channels is presented.

The printer that was mentioned in previous chapters, twelve channel HP DesignJet Z3200, was now employed. The reason that it was not used in modeling process was time that it took us to get the corresponding RIP. Nevertheless, in this part of thesis it was crucial element because of its much better gamut size comparing to the four channel printers. The gamut of the HP DesignJet Z3200 printer was obtained for five different papers and visualized using ICC3D. Calibration process of the HP DesignJet Z3200 printer results with a printed color chart made of a ramps for each channel. These ramps were then measured manually with Eye One Pro spectrophotometer because of the specific hexagonal shape of color patches. Linear testchart was also measured with the same spectrophotometer and then spectral reflectances obtained with it were compared with

the ones obtained with Spectrolino. The RMSE for these two measurements was then calculated to be 0.001. For this reason representing and comparing gamut values for four colorant printers with HP DesignJet Z3200 was continued to be done with certainty of precision [59] [59].

5.5 Proposed Algorithm

With the change of the paper substrate the diversity of possible spectral print reproduction was goal to be checked. The fact that in process of reaching final confirmation or negation of spectral print possibility many different steps are conducted it was very important to make that process decreased in time consumed [60] [61] [58]. In this particular case there were 32 spectral data color samples given for which feasibility was to be checked. Nevertheless, as mentioned before, that was just the subset of initial amount wanted to be reproduced in form of spectral print. For that reason the algorithm that enables the whole process, from spectral reflectance input to final decision of sending to printer or not, automated was proposed.
At the beginning of the proposed algorithm the input data required was the spectral reflectance data measurements. It needs to be noted here that it is important take care of the geometry of measurements for the main goal. When (if) spectral print reproduction of wanted object was confirmed to be feasible the final print reproduction should be measured under same conditions, geometry and illuminats. Since the next step was mapping the color gamut of a initial values to the gamut given by output mechanism, printer, the values were represented with an image. For the image format Tagged Image File Format was chosen. TIFF image format enables data obtained from spectral reflectances measured under certain illuminant to be presented separately for each of L*, a* and b* channels. If this wanted to be replaced with CMYK values TIFF is again the best choice because in that case it represents four channels separately. By use of TIFF format the conversion to RGB space was skipped, regarding important use of displays, during the whole process. This helps in making the whole process faster and simple. After the TIFF image was created in CIELAB color space next step was to map that image file, which is the representation of the spectral reflectance of the object wanted to be printed, to the gamut of a printed for a certain paper. In process of mapping ICC3D software was employed and constrains set was minimum delta and constant hue in order to achieve the best perceptual match of final reproduction. Obtained mapped image is again in TIFF format [62] which enables to extract the L*, a* and b* channel data. Next, that data was used in step of comparing the differences between the initial TIFF image and mapped TIFF image. Then the calculation of the differences for several color spaces in case of several paper substrates under different illuminants was done. Visualization of the points that are out of gamut for a certain paper was presented in order to be able to notice which part of gamut should be considered to be extended if possible was the next step done. Finally, with the constraints to be considered, i.e. value more than 1.2 for delta CMC overcomes the aim, the spectral color points were confirmed or not to be feasible to print within the gamut possibilities for specific combination of colorants/paper of printer given. The feasibility of the defined input data from retailer was then tested with this proposed method for five different papers. The scheme can be seen in fig. 35.

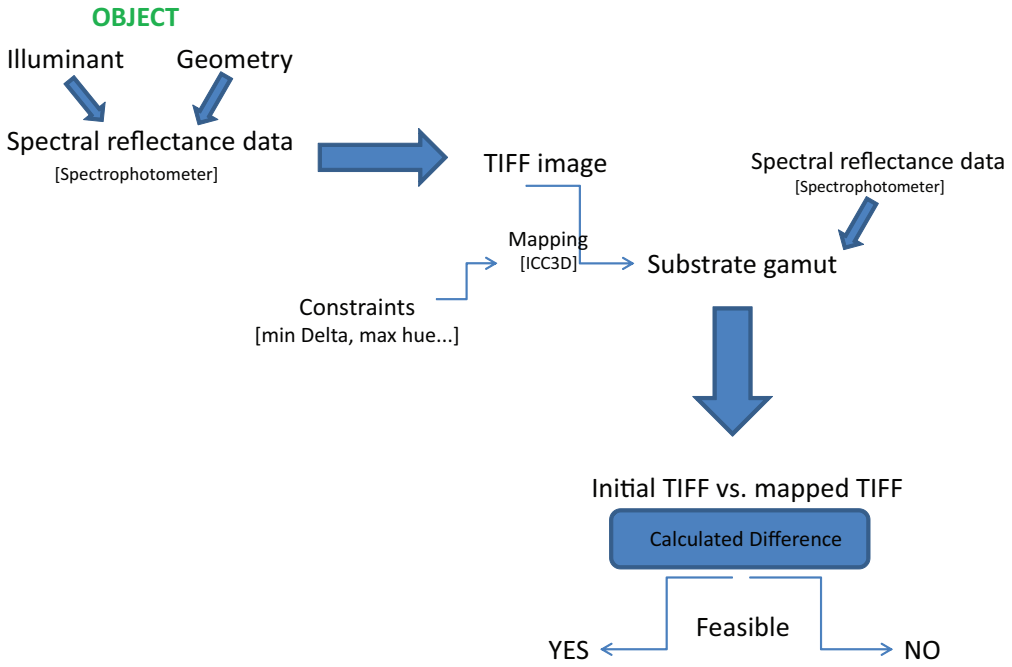

Figure 35: Feasibility of spectral print reproduction algorithm scheme.

5.6 HP Heavy Coated paper

A	HP Heavy Coated paper											
	ΔE			Δ94			ΔCMC			ΔE00		
	min	max	avg	min	max	avg	min	max	avg	min	max	avg
D50	0,21	11,38	2,41	0,15	10,56	1,98	0,21	18,82	2,66	0,17	7,65	1,57
D65	0,21	11,02	2,48	0,15	10,17	2,02	0,21	18,12	2,68	0,17	7,37	1,60
A	0,26	11,02	2,45	0,11	10,49	1,99	0,13	18,77	2,80	0,10	7,54	1,58
C	0,26	11,02	2,50	0,20	12,96	2,83	0,13	18,77	2,85	0,10	7,54	1,62
F2	0,21	16,13	4,02	0,20	12,96	2,83	0,28	16,67	3,35	0,21	8,84	2,30
UL3000	0,21	16,13	4,07	0,20	12,96	2,87	0,28	17,37	3,42	0,21	8,84	2,33

Figure 36: Results of gamut mapping to paper A given with different color differences equations under 6 illuminants.

The paper that the testing the feasibility was started with was HP Heavy Coated paper. That paper is $130 g/m^2$ paper often used while high quality print reproduction is to be obtained. From the fig. 36 the calculations can be read. The important results form the table given are the one for CMC color difference under UL3000 illuminant. This is the determination point of spectral print feasibility. As stated in problem given the spectral print should match under illuminant UL3000 but the rest illuminants match is highly desirable. For that reason the other illuminants (D50,D65,A,C,F2) were taken into account. In this particular case the input spectral reflectance data come from the cloth object which is the reason of delta CMC being important. Nevertheless, a few other color differences were employed as well to see how the resulting calculations behave in different mathematical color environment. This is also due to the fact that the algorithm can

be used not only for spectral data obtained from measuring the garnament but the variety of objects and products. In this particular case of paper it can be seen that the minimum CMC difference is obtained under illuminnat different than UL3000 but even for the aimed illuminant the results are satisfied. This is in case of minimum but if the average is to be read, the 1.8 and 0.8 threshold values become overpassed. This can be misleading number because the significant amount of samples is still above 1.2 values and 0.8. This can be seen from the histogram in fig. 37. From there is easier to observe the amount of samples that are feasible to be produced in spectral print reproduction, in particular 13 samples are under CMC 0.8 value and 6 under CMC 1.2 value of total 32 samples.

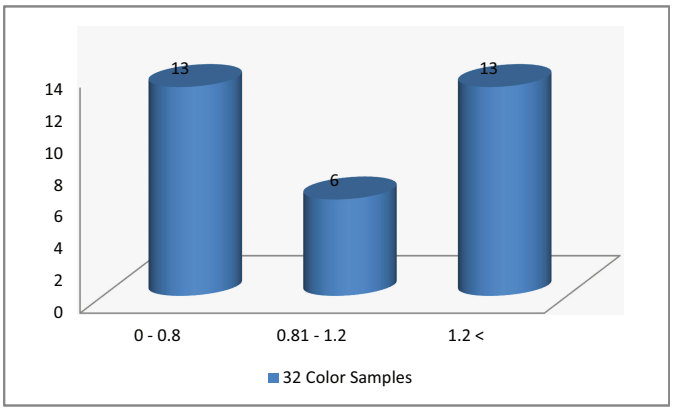

Figure 37: Histogram of resulting CMC difference for 32 color samples mapped to printer gamut on paper A.

In observing the values that go over the 1.2 CMC value, the particular color points that are the most far away from wanted values to be mapped are in yellow and dark blue(black) part of the color gamut that can be seen from the fig. 38. This is the crucial information where to look for gamut extension in order to achieve the wanted spectral reproduction.

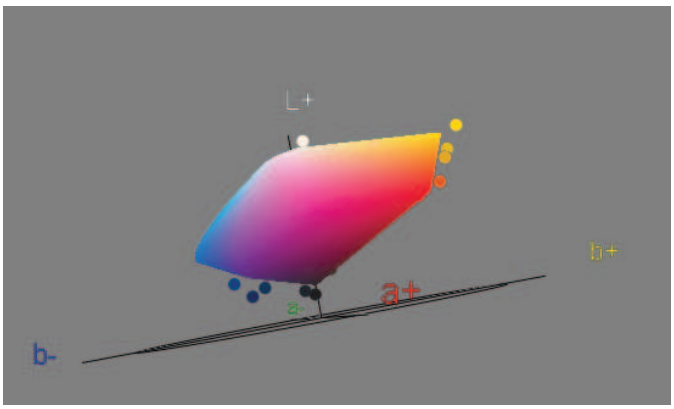

Figure 38: Visualization of initial color values and gamut of print created with paper A before mapping, in 3D space.

In the end, starting from the intimal 3 separated channels in TIFF format the mapped version to gamut obtained on HP Heavy Coated paper is created and presented visually with L*a*b* values in color ramp of target colors with the fig. 39

Figure 39: Color samples mapped to gamut of HP Heavy Coated paper under illuminant UL3000 for 10 degree observer.

5.7 HP Professional Matte Canvas

The HP Professional Matte Canvas is $430 g/m^2$ paper often for fine art reproduction. This paper was chosen for the texture that resembles more to the cloth that the HP Heavy Coated paper. In this particular case of paper it can be seen from the fig. 40 that the maximum CMC difference is obtained under illuminat different than UL3000 but even for the aimed illuminant the results are satisfied. This is in case of minimum but if the average is to be read, the 1.8 and 0.8 threshold values become overpassed. This is again, as mentioned before, misleading number because the significant amount of samples is still above 1.2 values and 0.8. This can be seen from the histogram in fig. 41. From there is easier to observe the amount of samples that are feasible to be produced in spectral print reproduction, in particular 20 samples are under CMC 0.8 value and 5 under CMC 1.2 value of total 32 samples. In observing the values that go over the 1.2 CMC

B	HP Professional Matte Canvas											
	ΔE			Δ94			ΔCMC			ΔE00		
	min	max	avg	min	max	avg	min	max	avg	min	max	avg
D50	0,21	11,02	1,96	0,11	10,49	1,63	0,13	18,77	2,50	0,10	7,54	1,28
D65	0,21	10,65	2,01	0,11	10,11	1,66	0,13	18,07	2,51	0,10	7,25	1,31
A	0,21	11,02	2,41	0,11	10,49	1,91	0,13	18,77	2,68	0,10	7,54	1,54
C	0,21	10,65	1,98	0,11	10,11	1,64	0,13	18,07	2,49	0,10	7,25	1,30
F2	0,21	11,25	3,11	0,20	9,69	2,41	0,28	16,67	3,11	0,21	8,02	1,96
UL3000	0,21	10,28	2,04	0,11	9,72	1,69	0,13	17,37	2,52	0,10	6,96	1,33

Figure 40: Results of gamut mapping to paper B given with different color differences equations under 6 illuminants.

value, the particular color points that are the most far away from wanted values to be mapped are in yellow and dark blue(black) part of the color gamut that can be seen from the fig. 42. This is the crucial information where to look for gamut extension in order to achieve the wanted spectral reproduction.

Again, starting from the intimal 3 separated channels in TIFF format the mapped version to gamut obtained on HP Professional Matte Canvas is created and presented visually with L*a*b* values in color ramp of target colors with the fig. 43

5.8 HP Artist Matte Canvas

The HP Artist Matte Canvas is $380 g/m^2$ paper often for fine art reproduction. This paper was chosen for the texture that resembles even more to the cloth that the HP Professional Matte Canvas. In this particular case of paper it can be seen from the fig. 44 that the maximum CMC

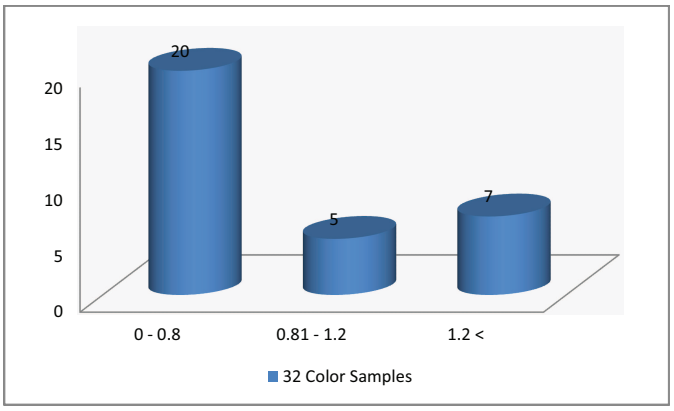

Figure 41: Histogram of resulting CMC difference for 32 color samples mapped to printer gamut on paper B.

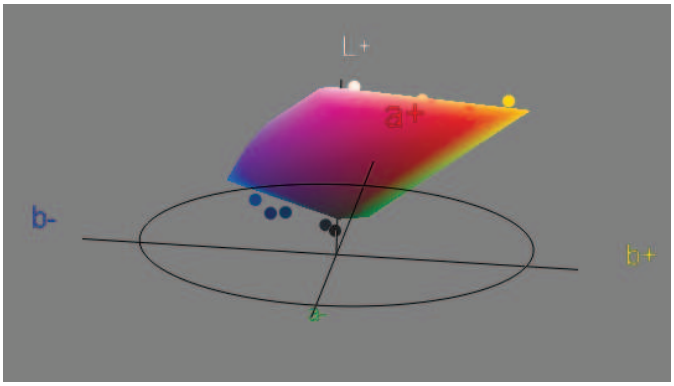

Figure 42: Visualization of initial color values and gamut of print created with paper B before mapping, in 3D space.

Figure 43: Color samples mapped to gamut of HP Professional Matte Canvas under illuminant UL3000 for 10 degree observer.

difference is obtained under illuminnat UL3000 so in comparison with the rest illuminants the calculations obtained are satisfied. This is in case of minimum but if the average is to be read, the 1.8 and 0.8 threshold values become overpassed. This is again, as mentioned before, misleading number because the significant amount of samples is still above 1.2 values and 0.8. This can be seen from the histogram in fig. 45. From there is easier to observe the amount of samples that are feasible to be produced in spectral print reproduction, in particular 20 samples are under CMC 0.8 value and 5 under CMC 1.2 value of total 32 samples. In observing the values that go over the 1.2 CMC value, the particular color points that are the most far away from wanted values to be mapped are in yellow and dark blue(black) part of the color gamut that can be seen

C	HP Artist Matte Canvas											
	ΔE			Δ94			ΔCMC			ΔE00		
	min	max	avg	min	max	avg	min	max	avg	min	max	avg
D50	0,21	11,02	2,45	0,11	10,49	1,96	0,13	18,77	2,73	0,10	7,54	1,57
D65	0,21	10,65	1,91	0,11	10,11	1,56	0,13	18,07	2,39	0,13	7,25	1,26
A	0,21	11,02	2,47	0,11	10,49	1,97	0,13	17,05	2,73	0,10	7,54	1,58
C	0,21	11,04	2,47	0,11	10,50	1,97	0,13	17,77	2,73	0,10	7,50	1,58
F2	0,21	11,02	3,31	0,20	10,49	2,50	0,28	18,77	3,19	0,21	7,54	2,02
UL3000	0,21	10,28	1,93	0,11	9,72	1,57	0,13	17,37	2,36	0,10	6,96	1,27

Figure 44: Results of gamut mapping to paper C given with different color differences equations under 6 illuminants.

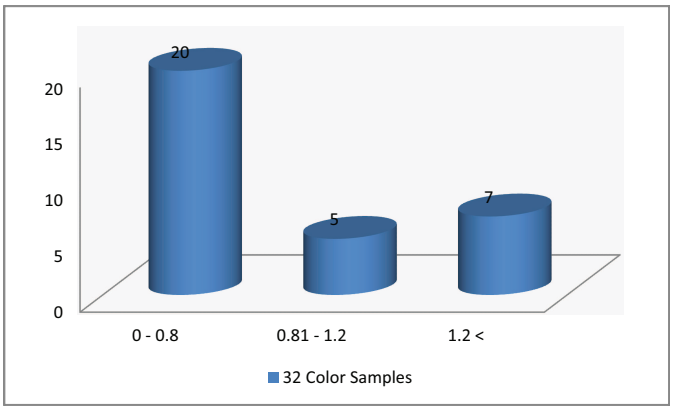

Figure 45: Histogram of resulting CMC difference for 32 color samples mapped to printer gamut on paper C.

from the fig. 46. From here the lead to direction to look for gamut extension in order to achieve the wanted spectral reproduction is created.

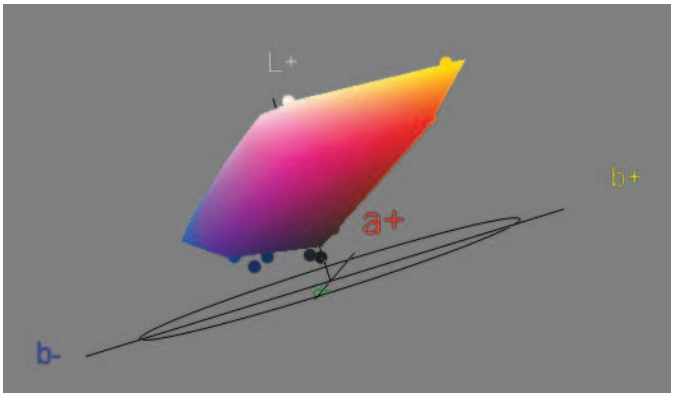

Figure 46: Visualization of initial color values and gamut of print created with paper C before mapping, in 3D space.

Again, starting from the intimal 3 separated channels in TIFF format the mapped version to

gamut obtained on HP Artist Matte Canvas is created and presented visually with L*a*b* values in color ramp of target colors with the fig. 47

Figure 47: Color samples mapped to gamut of HP Artist Matte Canvas under illuminant UL3000 for 10 degree observer.

5.9 HP Universal Coated Paper

The HP Universal Coated Paper is $95g/m^2$ paper often for universal print reproduction. This paper was chosen for establishing the relation between specific requirements with universal paper substrate in order to see the behavior in daily print materials.In this particular case of paper it can be seen from the fig. 48 that the maximum CMC difference is obtained under illuminnat UL3000 so in comparison with the rest illuminants the calculations obtained are satisfied. This is in case of minimum but if the average is to be read, the 1.8 and 0.8 threshold values become overpassed. This is again, as mentioned before, misleading number because the significant amount of samples is still above 1.2 values and 0.8. This can be seen from the histogram in fig. 49. From there is easier to observe the amount of samples that are feasible to be produced in spectral print reproduction, in particular 18 samples are under CMC 0.8 value and 6 under CMC 1.2 value of total 32 samples. In observing the values that go over the 1.2 CMC value,

D	HP Universal Coated Paper											
	ΔE			Δ94			ΔCMC			ΔE00		
	min	max	avg	min	max	avg	min	max	avg	min	max	avg
D50	0,21	12,47	2,41	0,15	11,72	2,02	0,21	20,92	2,82	0,17	8,52	1,60
D65	0,21	12,16	2,42	0,15	11,02	1,97	0,21	19,57	2,52	0,17	8,09	1,59
A	0,21	12,51	3,14	0,20	11,40	2,39	0,28	20,27	2,90	0,21	8,37	1,92
C	0,21	12,16	2,33	0,15	11,02	1,91	0,21	19,57	2,47	0,17	8,09	1,54
F2	0,21	14,79	3,55	0,20	13,26	2,64	0,28	17,42	3,00	0,21	9,27	2,17
UL3000	0,21	11,82	2,24	0,15	10,64	1,82	0,21	18,87	2,36	0,17	7,80	1,47

Figure 48: Results of gamut mapping to paper D given with different color differences equations under 6 illuminants.

the particular color points that are the most far away from wanted values to be mapped are in yellow and dark blue(black) part of the color gamut that can be seen from the fig. 50. From here the lead to direction to look for gamut extension in order to achieve the wanted spectral reproduction is created. Again, starting from the intimal 3 separated channels in TIFF format the mapped version to gamut obtained on HP Artist Matte Canvas is created and presented visually with L*a*b* values in color ramp of target colors with the fig. 51

5.10 HP Recycled Bond Paper

The HP Recycled Bond Paper is $80g/m^2$ paper often for low print reproduction. This paper was chosen for establishing the realtion between specific requirments with the paper substrate supporting the green technologies.This was to check the results with taking into account the future possibility of spectral print reproduction on reused paper substrate and in that way making it

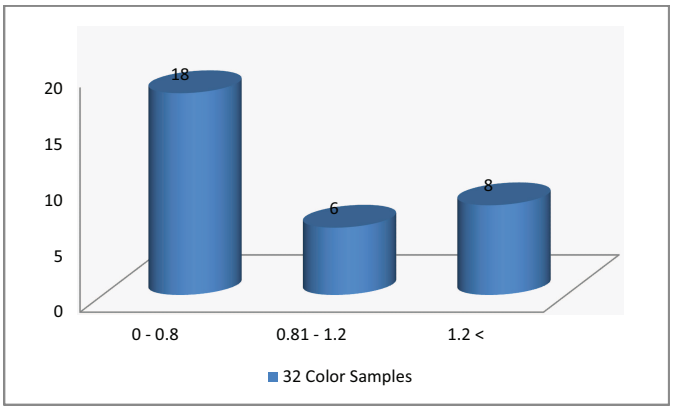

Figure 49: Histogram of resulting CMC difference for 32 color samples mapped to printer gamut on paper D.

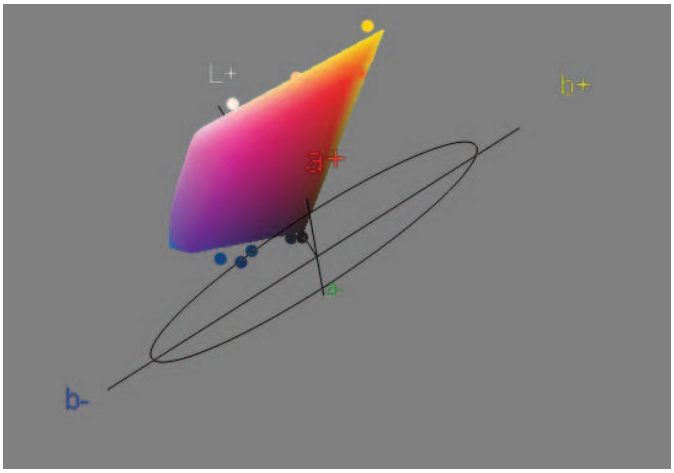

Figure 50: Visualization of initial color values and gamut of print created with paper D before mapping, in 3D space.

Figure 51: Color samples mapped to gamut of HP Universal Coated Paper under illuminant UL3000 for 10 degree observer.

more affordable and desirable for environment.In this particular case of paper it can be seen from the fig. 52 that the maximum CMC difference is obtained under illuminnat UL3000 so in comparison with the rest illuminants the calculations obtained are satisfied. This is in case of minimum but if the average is to be read, the 1.8 and 0.8 threshold values become overpassed. This is again, as mentioned before, misleading number because the significant amount of samples is still above 1.2 values and 0.8. This can be seen from the histogram in fig. 53. From there is easier to observe the amount of samples that are feasible to be produced in spectral print re-

production, in particular 7 samples are under CMC 0.8 value and 3 under CMC 1.2 value of total 32 samples. From these results it can be concluded that quality of the paper strongly affects the feasibility of the spectral print reproduction. In observing the values that go over the 1.2 CMC

E	HP Recycled Bond paper											
	ΔE			Δ94			ΔCMC			ΔE00		
	min	max	avg	min	max	avg	min	max	avg	min	max	avg
D50	0,26	22,44	7,82	0,21	19,70	5,23	0,28	34,64	6,74	0,25	14,98	4,30
D65	0,26	22,56	7,86	0,21	19,32	5,17	0,28	33,95	6,66	0,25	14,67	4,25
A	0,26	24,48	8,53	0,21	19,83	5,58	0,28	34,71	7,13	0,25	15,17	4,62
C	0,26	22,11	7,64	0,21	19,32	5,06	0,28	33,95	6,55	0,25	14,67	4,16
F2	0,26	30,78	10,09	0,24	18,41	6,15	0,33	32,47	7,61	0,29	14,07	5,10
UL3000	0,26	22,57	7,57	0,21	18,79	5,06	0,28	33,16	6,54	0,25	14,38	4,16

Figure 52: Results of gamut mapping to paper E given with different color differences equations under 6 illuminants.

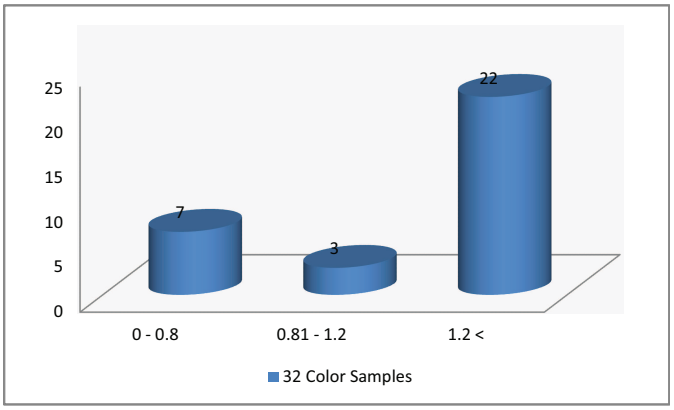

Figure 53: Histogram of resulting CMC difference for 32 color samples mapped to printer gamut on paper E.

value, the particular color points that are the most far away from wanted values to be mapped are in yellow and dark blue(black) part of the color gamut that can be seen from the fig. 54. From here the lead to direction to look for gamut extension in order to achieve the wanted spectral reproduction is created. Starting from the intimal 3 separated channels in TIFF format the mapped version to gamut obtained on HP Artist Matte Canvas is created and presented visually with L*a*b* values in color ramp of target colors with the fig. 55

5.11 Comparing results

After all substrates were tested and the feasibility was given with the results obtained the comparison of the five papers was done. This can be seen from the histogram in fig. 56. The fact that calculating the average difference from the ramp of target set of colors to be spectrally reproduced is not giving the correct answer need to be noted. For that reason histogram representation was used for more thorough conclusions about the feasibility. This move brings the improvement to visual representation of the data as well as to the calculation results. Finally,

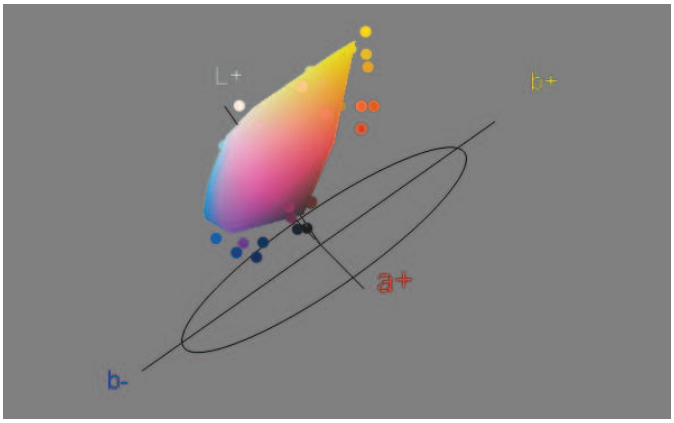

Figure 54: Visualization of initial color values and gamut of print created with paper E before mapping, in 3D space.

Figure 55: Color samples mapped to gamut of HP Recycled Bond Paper under illuminant UL3000 for 10 degree observer.

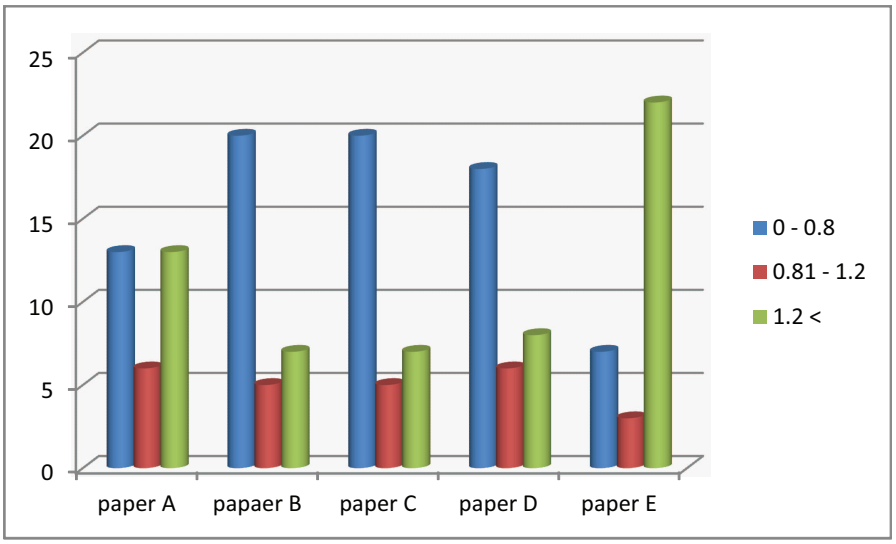

Figure 56: Histogram of resulting CMC difference for initial 32 color samples mapped to printer gamut on papers A,B,C,D and E.

all of the mapped values are given with the L*a*b* values that are possible to be reproduced. Observing it carefully gives the opportunity to apply the 3 visualization of gamuts to real samples wherease the wanted extension of gamut in yellow and blue (black) direction of gamut space is as well noticed. If focused on the yellow and blue samples of given ramp the deviation from the

initial ramp can be seen even with the bare eye. It is somewhat more difficult to noticed yellow mapped samples difference that blue ones due to ability of human visual system.

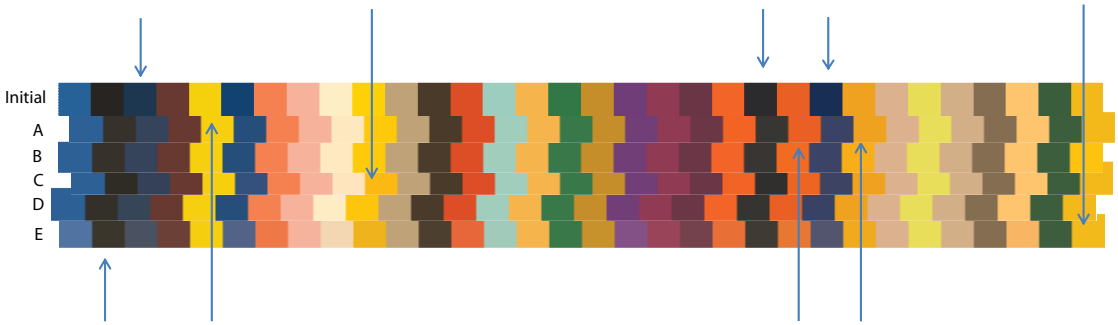

Figure 57: Color samples mapped to gamut of five different papers under illuminant UL3000 for 10 degree observer. The arrows point the samples most affected with the gamut mapping. Initial L*a*b* values are given in top ramp followed by papers A,B,C,D,and E towards the bottom. The arrows point the samples most affected with the gamut mapping.

6 Conclusion

During the work on this master thesis two questions that were initially stated were aimed to be answered. In order to successfully model the printer for final goal of spectral reproduction of garnament the Kubelka-Munk theory was employed for estimation of the Neugebauer primaries. This was done in order of saving time and resources. Combination of both measured and estimated spectral reflectances was also employed in testing the models. Further more, Kubelka-Munk equation was first time used for testing the cellular extension of spectral Neugebauer model and Yule-Nielsen spectral Neugebauer model. This resulted in even more accurate values of models tested. In the future work making the cell even smaller than only 0.5 of the unity should give even more better and accurate results.
In the second part of the thesis focus was on the feasibility of the spectral print reproduction. For that reason many different steps were included in one resulting algorithm. With this proposed method the whole process should be decreased in time for the bigger amount of data as input. The twelve colorant printer was tested for given target and that resulted with some deviations from wanted spectral print. This way it was possible to see exact which part of the gamut is lacking in contribution of the spectral print. The feasibility check was done for the primaries of the printer and this could be done with checking the overlaps of its primaries by estimating the secondaries, tertiaries and so on. This is step that is being worked on, yet due to deadline given the results are not presented here. The main drawback and one of the challenge to improve the algorithm is making it possible not only for the integer CIELAB values as input.

7 APPENDIX A

Results of mapping obtained with paper A (HP Heavy Coated paper) under different illuminats.

Figure 58: Color samples mapped to gamut of HP Heavy Coated paper under illuminant D50 for 10 degree observer.

Figure 59: Color samples mapped to gamut of HP Heavy Coated paper under illuminant D65 for 10 degree observer.

Figure 60: Color samples mapped to gamut of HP Heavy Coated paper under illuminant A for 10 degree observer.

Figure 61: Color samples mapped to gamut of HP Heavy Coated paper under illuminant C for 10 degree observer.

Figure 62: Color samples mapped to gamut of HP Heavy Coated paper under illuminant F2 for 10 degree observer.

Results of mapping obtained with paper B (HP Professional Matte Canvas) under different illuminats.

Figure 63: Color samples mapped to gamut of HP Professional Matte Canvas under illuminant D50 for 10 degree observer.

Results of mapping obtained with paper C (HP Artist Matte Canvas) under different illuminats.

Figure 64: Color samples mapped to gamut of HP Professional Matte Canvas under illuminant D65 for 10 degree observer.

Figure 65: Color samples mapped to gamut of HP Professional Matte Canvas under illuminant A for 10 degree observer.

Figure 66: Color samples mapped to gamut of HP Professional Matte Canvas under illuminant C for 10 degree observer.

Figure 67: Color samples mapped to gamut of HP Professional Matte Canvas under illuminant F2 for 10 degree observer.

Figure 68: Color samples mapped to gamut of HP Artist Matte Canvas under illuminant D50 for 10 degree observer.

Figure 69: Color samples mapped to gamut of HP Artist Matte Canvas under illuminant D65 for 10 degree observer.

Figure 70: Color samples mapped to gamut of HP Artist Matte Canvas under illuminant A for 10 degree observer.

Figure 71: Color samples mapped to gamut of HP Artist Matte Canvas under illuminant C for 10 degree observer.

Figure 72: Color samples mapped to gamut of HP Artist Matte Canvas under illuminant F2 for 10 degree observer.

Results of mapping obtained with paper D (HP Artist Matte Canvas) under different illuminats.

Results of mapping obtained with paper E (HP Recycled Bond Paper) under different illumi-

Figure 73: Color samples mapped to gamut of HP Artist Matte Canvas under illuminant D50 for 10 degree observer.

Figure 74: Color samples mapped to gamut of HP Universal Coated Paper under illuminant D65 for 10 degree observer.

Figure 75: Color samples mapped to gamut of HP Universal Coated Paper under illuminant A for 10 degree observer.

Figure 76: Color samples mapped to gamut of HP Universal Coated Paper under illuminant C for 10 degree observer.

Figure 77: Color samples mapped to gamut of HP Universal Coated Paper under illuminant F2 for 10 degree observer.

nats.

Figure 78: Color samples mapped to gamut of HP Recycled Bond Paper under illuminant D50 for 10 degree observer.

Figure 79: Color samples mapped to gamut of HP Recycled Bond Paper under illuminant D65 for 10 degree observer.

Figure 80: Color samples mapped to gamut of HP Recycled Bond Paper under illuminant A for 10 degree observer.

Figure 81: Color samples mapped to gamut of HP Recycled Bond Paper under illuminant C for 10 degree observer.

Figure 82: Color samples mapped to gamut of HP Recycled Bond Paper under illuminant F2 for 10 degree observer.

8 APPENDIX B

	Initial			Mapped		
Name	L	a	b	L	a	b
BLUE I	39,39	-1,15	-49,35	39,21569	0	-48
BLACK	12,91	0,09	-2,09	17,64706	0	0
BLUE II	21,01	-0,22	-28,03	27,05882	0	-25
CHERRY	28,05	19,97	9,29	28,23529	20	9
YELLOW	84,57	-5,08	80,11	84,70588	-4	80
BLUE III	25,91	3,1	-43,59	31,76471	2	-41
CORAL	68,38	43,07	40,52	60,39216	39	37
CORAL II	79,49	19,51	7,72	79,21569	19	7
CREMA	95,47	1,98	7,34	90,58824	1	6
YELLOW II	89,27	10,82	89,64	76,47059	9	80
DUNE	68,81	2,98	14,59	68,62745	3	15
BROWN	24,87	4,13	8,96	24,70588	4	9
RED	51,86	54,02	51,33	48,62745	49	46
BLUE IV	79,3	-19,86	-13,76	78,82353	-18	-12
YELLOW III	78	12,32	51,77	78,03922	12	52
GREEN	45,55	-34,29	14,42	45,4902	-33	14
YELLOW IV	62,69	10,51	54,2	62,7451	11	54
PURPLE	33,79	33,39	-37,37	33,72549	33	-36
MAGENTA	36,82	40,09	-5,46	36,86275	40	-4
MAGENTA II	28,67	25,6	-7,4	28,62745	26	-6
RED I	61,51	52,68	57,58	52,54902	44	48
BLUE V	15,71	0,19	-7,05	19,60784	0	-4
ORANGE	57,06	49,97	64,23	54,11765	41	53
PURPLE I	17,84	6,88	-35,55	27,45098	6	-32
YELLOW V	72,49	15,56	79,09	71,76471	15	76
PINK	75,65	8,51	12,21	75,68627	9	12
GREEN I	86,83	-14,48	53,93	86,66667	-13	54
BROWN I	74,02	6,3	12,7	74,11765	6	13
BLACK I	47,27	4,83	10,09	47,45098	5	10
RED II	84,75	13,9	41,72	79,60784	13	40
GREEN II	35,83	-23,17	8,81	35,68627	-22	9
YELLOW VI	78,19	5,52	83,84	78,03922	6	84

Figure 83: CIELAB values of the target and mapped to gamut created with paper A for UL300 illuminant and 10 degrees observer

	Initial			Mapped		
Name	L	a	b	L	a	b
BLUE I	39,39	-1,15	-49,35	39,21569	0	-48
BLACK	12,91	0,09	-2,09	19,21569	0	0
BLUE II	21,01	-0,22	-28,03	27,84314	0	-24
CHERRY	28,05	19,97	9,29	28,23529	20	9
YELLOW	84,57	-5,08	80,11	84,70588	-4	80
BLUE III	25,91	3,1	-43,59	31,76471	2	-41
CORAL	68,38	43,07	40,52	68,23529	43	41
CORAL II	79,49	19,51	7,72	79,60784	20	8
CREMA	95,47	1,98	7,34	93,33333	2	7
YELLOW II	89,27	10,82	89,64	82,7451	10	88
DUNE	68,81	2,98	14,59	68,62745	3	15
BROWN	24,87	4,13	8,96	24,70588	4	9
RED	51,86	54,02	51,33	51,76471	54	51
BLUE IV	79,3	-19,86	-13,76	79,21569	-19	-13
YELLOW III	78	12,32	51,77	78,03922	12	52
GREEN	45,55	-34,29	14,42	45,4902	-33	14
YELLOW IV	62,69	10,51	54,2	62,7451	11	54
PURPLE	33,79	33,39	-37,37	33,72549	33	-36
MAGENTA	36,82	40,09	-5,46	36,86275	40	-4
MAGENTA II	28,67	25,6	-7,4	28,62745	26	-6
RED I	61,51	52,68	57,58	61,56863	53	58
BLUE V	15,71	0,19	-7,05	20,78431	0	-4
ORANGE	57,06	49,97	64,23	57,2549	50	64
PURPLE I	17,84	6,88	-35,55	27,45098	6	-32
YELLOW V	72,49	15,56	79,09	72,54902	16	79
PINK	75,65	8,51	12,21	75,68627	9	12
GREEN I	86,83	-14,48	53,93	86,66667	-13	54
BROWN I	74,02	6,3	12,7	74,11765	6	13
BLACK I	47,27	4,83	10,09	47,45098	5	10
RED II	84,75	13,9	41,72	84,70588	14	42
GREEN II	35,83	-23,17	8,81	35,68627	-22	9
YELLOW VI	78,19	5,52	83,84	78,03922	6	84

Figure 84: CIELAB values of the target and mapped to gamut created with paper B for UL300 illuminant and 10 degrees observer

	Initial			Mapped		
Name	L	a	b	L	a	b
BLUE I	39,39	-1,15	-49,35	39,21569	0	-48
BLACK	12,91	0,09	-2,09	18,03922	0	0
BLUE II	21,01	-0,22	-28,03	27,45098	0	-24
CHERRY	28,05	19,97	9,29	28,23529	20	9
YELLOW	84,57	-5,08	80,11	84,70588	-4	80
BLUE III	25,91	3,1	-43,59	31,76471	2	-41
CORAL	68,38	43,07	40,52	68,23529	43	41
CORAL II	79,49	19,51	7,72	79,60784	20	8
CREMA	95,47	1,98	7,34	94,5098	1	6
YELLOW II	89,27	10,82	89,64	83,92157	10	89
DUNE	68,81	2,98	14,59	68,62745	3	15
BROWN	24,87	4,13	8,96	24,70588	4	9
RED	51,86	54,02	51,33	51,76471	54	51
BLUE IV	79,3	-19,86	-13,76	79,21569	-19	-13
YELLOW III	78	12,32	51,77	78,03922	12	52
GREEN	45,55	-34,29	14,42	45,4902	-33	14
YELLOW IV	62,69	10,51	54,2	62,7451	11	54
PURPLE	33,79	33,39	-37,37	33,72549	33	-36
MAGENTA	36,82	40,09	-5,46	36,86275	40	-4
MAGENTA II	28,67	25,6	-7,4	28,62745	26	-6
RED I	61,51	52,68	57,58	61,56863	53	58
BLUE V	15,71	0,19	-7,05	20	0	-4
ORANGE	57,06	49,97	64,23	57,2549	50	64
PURPLE I	17,84	6,88	-35,55	27,45098	6	-32
YELLOW V	72,49	15,56	79,09	72,54902	16	79
PINK	75,65	8,51	12,21	75,68627	9	12
GREEN I	86,83	-14,48	53,93	86,66667	-13	54
BROWN I	74,02	6,3	12,7	74,11765	6	13
BLACK I	47,27	4,83	10,09	47,45098	5	10
RED II	84,75	13,9	41,72	84,70588	14	42
GREEN II	35,83	-23,17	8,81	35,68627	-22	9
YELLOW VI	78,19	5,52	83,84	78,03922	6	84

Figure 85: CIELAB values of the target and mapped to gamut created with paper C for UL300 illuminant and 10 degrees observer

	Initial			Mapped		
Name	L	a	b	L	a	b
BLUE I	39,39	-1,15	-49,35	39,21569	0	-48
BLACK	12,91	0,09	-2,09	15,68627	0	0
BLUE II	21,01	-0,22	-28,03	27,05882	0	-24
CHERRY	28,05	19,97	9,29	28,23529	20	9
YELLOW	84,57	-5,08	80,11	84,70588	-4	80
BLUE III	25,91	3,1	-43,59	33,33333	2	-39
CORAL	68,38	43,07	40,52	68,23529	43	41
CORAL II	79,49	19,51	7,72	79,60784	20	8
CREMA	95,47	1,98	7,34	92,15686	1	6
YELLOW II	89,27	10,82	89,64	80	10	87
DUNE	68,81	2,98	14,59	68,62745	3	15
BROWN	24,87	4,13	8,96	24,70588	4	9
RED	51,86	54,02	51,33	51,76471	54	51
BLUE IV	79,3	-19,86	-13,76	79,21569	-19	-13
YELLOW III	78	12,32	51,77	78,03922	12	52
GREEN	45,55	-34,29	14,42	45,4902	-33	14
YELLOW IV	62,69	10,51	54,2	62,7451	11	54
PURPLE	33,79	33,39	-37,37	33,72549	33	-36
MAGENTA	36,82	40,09	-5,46	36,86275	40	-4
MAGENTA II	28,67	25,6	-7,4	28,62745	26	-6
RED I	61,51	52,68	57,58	60,78431	52	57
BLUE V	15,71	0,19	-7,05	18,03922	0	-4
ORANGE	57,06	49,97	64,23	59,21569	49	63
PURPLE I	17,84	6,88	-35,55	28,23529	6	-30
YELLOW V	72,49	15,56	79,09	72,54902	16	79
PINK	75,65	8,51	12,21	75,68627	9	12
GREEN I	86,83	-14,48	53,93	86,66667	-13	54
BROWN I	74,02	6,3	12,7	74,11765	6	13
BLACK I	47,27	4,83	10,09	47,45098	5	10
RED II	84,75	13,9	41,72	83,92157	13	41
GREEN II	35,83	-23,17	8,81	35,68627	-22	9
YELLOW VI	78,19	5,52	83,84	78,03922	6	84

Figure 86: CIELAB values of the target and mapped to gamut created with paper D for UL300 illuminant and 10 degrees observer

	Initial			Mapped		
Name	L	a	b	L	a	b
BLUE I	39,39	-1,15	-49,35	47,45098	0	-43
BLACK	12,91	0,09	-2,09	21,17647	0	2
BLUE II	21,01	-0,22	-28,03	33,72549	0	-19
CHERRY	28,05	19,97	9,29	31,37255	18	8
YELLOW	84,57	-5,08	80,11	83,92157	-4	80
BLUE III	25,91	3,1	-43,59	41,56863	2	-34
CORAL	68,38	43,07	40,52	63,52941	41	39
CORAL II	79,49	19,51	7,72	79,21569	19	7
CREMA	95,47	1,98	7,34	87,84314	1	6
YELLOW II	89,27	10,82	89,64	76,86275	8	71
DUNE	68,81	2,98	14,59	68,62745	3	15
BROWN	24,87	4,13	8,96	26,27451	3	7
RED	51,86	54,02	51,33	58,82353	45	42
BLUE IV	79,3	-19,86	-13,76	78,43137	-18	-12
YELLOW III	78	12,32	51,77	78,03922	12	52
GREEN	45,55	-34,29	14,42	45,4902	-33	14
YELLOW IV	62,69	10,51	54,2	63,52941	10	53
PURPLE	33,79	33,39	-37,37	41,56863	30	-33
MAGENTA	36,82	40,09	-5,46	40,39216	38	-3
MAGENTA II	28,67	25,6	-7,4	33,33333	23	-5
RED I	61,51	52,68	57,58	60,78431	41	45
BLUE V	15,71	0,19	-7,05	23,13725	0	-1
ORANGE	57,06	49,97	64,23	62,35294	37	48
PURPLE I	17,84	6,88	-35,55	36,07843	5	-25
YELLOW V	72,49	15,56	79,09	74,5098	13	67
PINK	75,65	8,51	12,21	75,68627	9	12
GREEN I	86,83	-14,48	53,93	86,66667	-13	54
BROWN I	74,02	6,3	12,7	74,11765	6	13
BLACK I	47,27	4,83	10,09	47,45098	5	10
RED II	84,75	13,9	41,72	79,21569	13	40
GREEN II	35,83	-23,17	8,81	35,68627	-21	8
YELLOW VI	78,19	5,52	83,84	78,82353	5	74

Figure 87: CIELAB values of the target and mapped to gamut created with paper E for UL300 illuminant and 10 degrees observer

9 APPENDIX C

Hints in calculation process using Matlab.

```
%Inverse Murray–Davies for estimating effective coverage of each colorant

%%%%%%%%%%%%%%%%
%   C+M+Y+K    %
%%%%%%%%%%%%%%%%

o4_refl=o3_ramp;
r_paper=(o4_refl(57,5:40));
c100=o4_refl(1, 5:40);
m100=o4_refl(15, 5:40);
y100=o4_refl(29, 5:40);
k100=o4_refl(43, 5:40);

% CYAN Effective area
for i=1:14
    c_measured(i,:)=(o4_refl(i,5:40) - o4_refl(57,5:40));
end

R_t=(o4_refl(1, 5:40) - r_paper);

for i=1:14
    upper_c(i,:)=(c_measured(i,:)*R_t(1,:)');
end


R_tt=R_t';
lower_c= R_t*R_tt;

C_eff=upper_c./lower_c;
C_eff=C_eff(1:14,:);

% CMYK_eff = [C_eff(1:14,:)] ;

c_theo =o4_refl(1:14,1)/100;
figure(1)
plot(c_theo,C_eff,'c');

% MAGENTA Effective area
o4_refl_m=o4_refl(15:28,:);
for i=1:14
```

```
    m_measured(i,:)=(o4_refl_m(i,5:40) - o4_refl(57,5:40));
end


M_R_t=(o4_refl_m(1, 5:40) - r_paper);

for i=1:14
    upper_m(i,:)=(m_measured(i,:)*M_R_t(1,:)');
end


M_R_tt=M_R_t';
lower_m= M_R_t*M_R_tt;

M_eff=upper_m./lower_m;
M_eff=M_eff(1:14,:);

% CMYK_eff = [C_eff(1:30,:) M_eff(1:30,1) ] ;

m_theo =o4_refl(1:14,1)/100;
figure(2)
plot(m_theo,M_eff(1:14,1),'m');


% Yellow Effective area
o4_refl_y=o4_refl(29:42,:);
for i=1:14
    y_measured(i,:)=(o4_refl_y(i,5:40) - o4_refl(57,5:40));
end

y_measured = y_measured(1:14,:);
Y_R_t=(o4_refl_y(1, 5:40) - r_paper);

for i=1:14
    upper_y(i,:)=(y_measured(i,:)*Y_R_t(1,:)');
end


Y_R_tt=Y_R_t';
lower_y= Y_R_t*Y_R_tt;

Y_eff=upper_y./lower_y;
Y_eff=Y_eff(1:14,:);

% CMYK_eff = [C_eff(1:30,:) M_eff(1:30,1)  Y_eff(1:30,1)] ;


y_theo =o4_refl(1:14,1)/100;
figure(3)
```

```
plot(y_theo,Y_eff(1:14,1),'r');


% BLACK Effective area

o4_refl_k=o4_refl(43:56,:);
for i=1:14
    k_measured(i,:)=(o4_refl_k(i,5:40) - o4_refl(57,5:40));
end

k_measured = k_measured(1:14,:);
K_R_t=(o4_refl_k(1, 5:40) - r_paper);

for i=1:14
    upper_k(i,:)=(k_measured(i,:)*K_R_t(1,:)');
end


K_R_tt=K_R_t';
lower_k= K_R_t*K_R_tt;

K_eff=upper_k./lower_k;
K_eff=K_eff(1:14,:);
-----------------------------------------------------------

%testing Neugebauer model with the KM measured and estimated Oce & Xerox NPs

%loading illuminants and observer data
%loading Neugebauer primeries of our two printers and
%colorant concentration and reflectances of the test chart

NP = load('x3_eNP_KM.txt'); % for Xerox estimated NPs
NP = load('x3_mNP.txt'); % for Xerox measured NPs
NP = load('O4_eNPs.txt'); % for Oce estimated NPs
NP = load('O4_eNPs.txt'); % for Oce measured NPs


Mref = load('X3_tc.txt');
Mref = x3_tc(193:300,5:40);
C = x3_tc(193:300,1:4);
%Cc is interpolated with Eff_Coverage results


NP=NP';

for i=1:108
    ww (:,i)= demichel2(C(i,:)');
end
NP=NP';
```

```
for i=1:108
     ref(:,i) = NP*ww(:,i);
end

NP = NP';
for i=1:108
    ww = demichel2(C(i,:)');
    ref(:,i) = NP*ww;
end
Mref = Mref';
RMSE = calcRMSE(ref,Mref);
GFC = calcGFC(ref,Mref);
MRMSE = sum(RMSE)/108;
MGFC = sum(GFC)/108;

------------------------------------------------------------

%ESTIMATION of X3 ramps by MD using Effective Color Coverage
for i=1:14
r_est_c_eff(i,:)=(1-(c(i,1)/100))*r_paper+(c(i,1)/100)*r_maxcove;
end

% ESTIMATED Magenta ramps
for i=1:14
r_est_m_eff(i,:)=(1-(c(i,2)/100))*r_paper+(c(i,2)/100)*r_maxcove;
end

% ESTIMATED Yellow ramps
for i=1:14
r_est_y_eff(i,:)=(1-(c(i,3)/100))*r_paper+(c(i,3)/100)*r_maxcove;
end

% ESTIATED Black ramps
for i=1:14
r_est_k_eff(i,:)=(1-(c(i,4)/100))*r_paper+(c(i,4)/100)*r_maxcove;
end

------------------------------------------------------------

%testing YN-Neugebauer model with the KM estimated NPs
for paper = 1:5

    NP = load([paper{paperidx},'MNPs.txt']);
    Mref = load([paper{paperidx},'TC.txt']);
    Ramp = load([paper{paperidx},'Scale.txt']);
    NP = NP';

    ref = zeros(36,1504,51);
```

```
    for n=1:0.1:maxn;
        n;
        aeff = colcoverage(Ramp.^(1/n));
        for i=1:908
            ww = demichel2(aeff(i,:)');
            ref(:,i,uint8((n-0.9)*10)) = (NP.^(1/n)*ww).^n;
        end
    end

    Mref = Mref';

    n=length(1:0.1:maxn);

    for j= 1:n
        temp = ref(:,:,j);

            RMSE = calcRMSE(temp(3:33,:),Mref(3:33,:));
            GFC = calcGFC(temp(3:33,:),Mref(3:33,:));

        RMSEw{j} = RMSE;
        GFCw{j} = GFC;
    end
    for i=1:n
        ARMSE(:,i) = RMSEw{i}';
        AGFC(:,i) = GFCw{i}';
    end
        MRMSE = mean(ARMSE);
        stdRMSE = std(ARMSE);
        maxRMSE = max(ARMSE);

        MGFC = mean(AGFC);
        stdGFC = std(AGFC);
        minGFC = min(AGFC);


_____________________________________________________________________
jcp_lab =read(jcp_lab.txt);
jcp_lab3d=reshape(jcp_lab, 32,1,[]);
imwrite(jcp_lab3d, 'jcp_lab3d.tiff', 'tiff', 'Colorspace','cielab','Compression','nor
mapped=imread ('mapped_X', 'tiff');

% t = Tiff('mapped_A','r');
% [L a b] = t.read();
% L = double(L)*(100/255);
% a = double(a) - 128;
% b = double(b) - 128;
%imfinfo('mappedT','tiff');
%mapped_lab2d=reshape(mapped_lab3d, 33,3);
% final= icclab2cielab('mapped_lab2d');
```

```
% input_class = class('proba.tiff');
% S = char(input_class);
% C= double(input_class);
% D=double(C);

input_class = class(mapped);
cielab = double(mapped);

if strcmp(input_class, 'uint8')
    % Fix L* values.
    cielab(:,:,1) = cielab(:,1)/2.55;
    cielab(:,:,2) = cielab(:,2)-128;
    cielab(:,:,3) = cielab(:,3)-128;
end

 mapped2d=reshape(cielab, 32,3);
 mapped2d=double(mapped2d);

 for i=1:32
  DE(i)=dEcalc(jcp_lab(i,1:3),mapped2d(i,1:3));
  DE94(i) = CIE94(jcp_lab(i,1:3),mapped2d(i,1:3), 1, 1, 1);
  DCMC(i)=cmc(jcp_lab(i,1:3),mapped2d(i,1:3));
  DE00(i)=deltaE2000(jcp_lab(i,1:3),mapped2d(i,1:3));
 end


mapped_lab3d16=uint16(mapped_lab3d);
input_class = class(mapped_lab3d16);
cielab = double(mapped_lab3d16);

if strcmp(input_class, 'uint16')
    % Fix L* values.
    cielab(:,:,1) = cielab(:,:,1) * (65535/65280);

    % How much to shift the a* and b* values.
    shift_value = 32768;
else
    shift_value = 128;
end

if size(cielab,3) > 1
    % Fix a* and b* values.
    ab = cielab(:,:,[2 3]);

    % Shift low values up.
    mask = ab <= (shift_value - 1);
    ab(mask) = ab(mask) + shift_value;
```

```
    % Shift high values down.
    mask = ~mask;
    ab(mask) = ab(mask) - shift_value;

    cielab(:,:,[2 3]) = ab;
end

if strcmp(input_class, 'uint16')
    cielab = uint16(cielab);
else
    cielab = uint8(cielab);
end
```

Bibliography

[1] Assefa, M. Kubelka munk theory for efficient spectral printer modelling. Master's thesis, 2010.

[2] Blahov. Evaluating the use of mixed neugebauer primaries, measured and estimated by kubelka-munk theory, in spectral reproduction using spectral neugebauer model and yule-nielsen modification. Master's thesis.

[3] Balasubramanian, R. The use of spectral regression in modeling halftone color printers.

[4] Bugnon, T. & Hersch, R. D. Constrained acquisition of ink spreading curves from printed color images.

[5] Di-Yuan Tzeng, R. S. B. A review of principal component analysis and its applications to color technology.

[6] Je-Ho Lee, Member, I. & Jan P. Allebach, Fellow, I. Inkjet printer model-based halftoning.

[7] A guide to halftone technologies.

[8] Kipphan, H. 2001. *Handbook of Print Media: Technologies and Production Methods*.

[9] Murat Mese, P. P. V. Recent advances in digital halftoning and inverse halftoning methods.

[10] Balasubramanian, R. The use of spectral regression in modeling halftone color printers.

[11] Evans, B. L. Error diffusion halftoning methods forimage display.

[12] Derhak, M. Spectral print inversion strategies.

[13] M. J. Vrhel, H. J. T. Color printer characterization in matlab.

[14] Emmel, P., Amidror, I., Ostromoukhov, V., & Hersch, R. D. 2005. Predicting the spectral behaviour of colour printers for transparent inks on transparent support.

[15] Jeremie Gerhardt, J. Y. H. Spectral color reproduction minimizing spectral and perceptual color differences.

[16] Gerhardt, J. *Reproduction spectrale de la couleur: approches par modelisation dimprimante et par halftoning avec diffusion derreur vectorielle*. PhD thesis.

[17] Fabrice Rousselle, Thomas Bugnon, R. D. H. Spectral prediction model for variable dot-size printers.

[18] Hong-Kee Kim, Byoung-Ho Kang, G.-S. H. J.-S. K. A method of printer modeling with the spectral reflectance curves using error back propagation.

[19] Zuffi, S. & Schettini, R. 2004. Modeling dot gain and inks interaction. In *in Proc. IS&T/SID 12th Color Imaging Conference (IS&T*, 181–186.

[20] Zuffi, S., Schettini, R., & Mauri, G. 2005. Spectral-based printer modeling and characterization. *J. Electronic Imaging*, 14(2), 023008.

[21] Lawler. 1997. *Lawler*.

[22] Lewandowski, A., Ludl, M., Byrne, G., & Dorffner, G. Aug 2006. Applying the yule-nielsen equation with negative n. *J. Opt. Soc. Am. A*, 23(8), 1827–1834.

[23] Bastani, B. 2009. *Spectral analysis of output devices from printing to predicting, PhD thesis*.

[24] Lawrenece A. Taplin, R. S. b. Spectral color reproduction based on a six-colorant inkjet output system.

[25] Binyu Wang, Haisong Xu, M. R. L. & Guo, J. Spectral-based color separation method for a multi-ink printer.

[26] Urban, P. & Grigat, R.-R. 2006. Spectral-based color separation using linear regression iteration. *Color Research and Application*, 31(3), 229–238.

[27] Philipp Urban, M. R. R. R. S. B. Accelerating spectral-based color separation within the neugebauer subspace.

[28] Balasubramanian, R. A spectral neugebauer model for dot-on-dot printers.

[29] Roy S. Berns, Animesh Bose, D.-Y. T. The spectral modeling of large-format ink-jet printers.

[30] Raimondo Schettini, Daniela Bianucci, G. M.-S. Z. An empirical approach for spectral color printers characterization.

[31] Roger David Hersch, F. C. Improving the yule-nielsen modified spectral neugebauer model by dot surface coverages depending on the ink superposition conditions.

[32] Younda Chen, R. S. B. & Taplin, L. A. Six color printer characterization using an optimized cellular yule-nielsen spectral neugebauer model.

[33] Bastani, B., Cressman, B., Shaw, M., packard Company, H., & Poster, U. 1996. Sparse cellular neugebauer model for n-ink printers. In *Proc. IS&T/SID Fourth Color Imaging Conference: Color Science, Systems and Applications*, 58–60.

[34] D.R.Wyble, R. B. 2000. A critical review of spectral models applied to binary color printing.

[35] Rotea, M. & Lana, C. A robust estimation algorithm for printer modeling.

[36] Yongda Chen, Roy S. Berns, L. A. T. Extending printing color gamut by optimizing the spectral reflectance of inks.

[37] Akao, Y., Yamamoto, A., & Higashikawa, Y. 2009. Estimation of inkjet printer spur gear teeth number from pitch data string of limited length. In *Proceedings of the 3rd International Workshop on Computational Forensics*, IWCF '09, 25–32, Berlin, Heidelberg. Springer-Verlag.

[38] *The 9th Color Imaging Conference: Color Science and Engineering: Systems, Technologies, Applications, November 6, 2001, Scottsdale, Arizona, USA*. IS&T - The Society for Imaging Science and Technology, 2001.

[39] Binyu Wang, Haisong Xu, M. R. L. a. J. G. Maintaining accuracy of cellular yulenielsen spectral neugebauer models for different ink cartridges using principal component analysis.

[40] Song-hua Hea, Z. L. The linear colorant mixing space based on kubleka-munk turbid media theory.

[41] *Hunter l,a,b Color Scale*.

[42] Taplin, L. A. Spectral modeling of a six-color inkjet printer.

[43] Roy S. Berns, Francisco H. Imai, P. D. B. & Tzeng, D.-Y. Multi-spectral-based color reproduction research at the munsell color science laboratory.

[44] Mekides Abebe, J. G. & Hardeberg, J. Y. 2011. Kubelka-munk theory for efficient spectral printer modeling.

[45] Uribe, J. Understanding black point compensation.

[46] Tzeng, D.-Y. *SPECTRAL-BASED COLOR SEPARATION ALGORITHM DEVELOPMENT FOR MULTIPLE-INK COLOR REPRODUCTION*. PhD thesis.

[47] *Data Hiding in Halftone Images using Error Diffusion Halftoning with Adaptive Thresholding*, 2006.

[48] Bastani, B. *SPECTRAL ANALYSIS OF OUTPUT DEVICES, FROM PRINTING TO PREDICTING*. PhD thesis.

[49] Evans, B. L. How to make printed and displayed images have high visual quality.

[50] Shohei Tsutsumi, Mitchell R. Rosen, R. S. B. Spectral color management using interim connection spaces based on spectral decomposition.

[51] Bugnon, T. & Hersch, R. D. 2011. Illumination estimation via thin-plate spline interpolation. 28, 940–94.

[52] Richard L. Alfvin, M. D. F. Observer variability in metameric color matches using color reproduction media.

[53] Beretta, G. B. The labpqr color space.

[54] Nicolas Bonnier, Francis Schmitt, H. B. & Berche, S. Evaluation of spatial gamut mapping algorithms.

[55] Mitchell R. Rosen, M. W. D. Spectral gamuts and spectral gamut mapping.

[56] *Konica Minolta - Light sources and illuminants*.

[57] 2008, January. Introduction of cmc colour differneces, scoop.

[58] Farup, I. & Hardeberg, J. Y. Interactive color gamut mapping.

[59] In-Su Jang, Chang-Hwan Son, T.-Y. P. K.-W. K. & Ha, Y.-H. Hi-fi printer characterization method using color correlation for gamut extension.

[60] Rosen, M. R. & Ohta, N. 2003. Spectral color processing using an interim connection space. In *Color Imaging Conference*, 187–192.

[61] Balasubramanian, R. & Dalal, E. A method for quantifying the color gamut of an output device.

[62] Adobe photoshop tiff technical notes.

Feasibility of spectral print reproduction

Kristina Marijanovic
The Norwegian Color and
Media Computing Laboratory
Gjøvik University College,
Gjøvik, Norway
kristina.marijanovic@hig.no

Jon Yngve Hardeberg
The Norwegian Color and
Media Computing Laboratory
Gjøvik University College,
Gjøvik, Norway
jon.hardeberg@hig.no

ABSTRACT

Within this work answering to question of feasibility of spectral print reproduction of targeted natural object was aimed. From the world that surrounds us human visual system is able to sense much wider range of color than any output system is able to reproduce. Printing machines are part of that system with their own defined environment and communication channels and the real challenge is these to be overcame. Certain data with different kind of sensors describes the objects, in our case that data is defined with the spectrophotometers. Before sending any data to printing process in order to obtain spectral print the feasibility of that process should be confirmed. If neglecting that fact, hit-and-miss tries would yield big waste of time and energy. For that reason the automated process in verifying the feasibility of color sensation being printed spectrally of certain object was created.

Keywords

Spectral print reproduction, Gamut mapping, Spectral print feasibility automation

1. INTRODUCTION

The challenge of spectral print feasibility of target object was tried to be automated. Instead of several different steps in creation of that process, one unique was created and the new algorithm, which includes all the segments together, and that way saves time, was proposed. In this way big amount of input data can be initially placed and from the output it can be seen exact which parts of the gamut for targeted spectral reproduction are missing. The answer to set of the spectral print feasibility of number of objects, under the same illuminant, was given. With the change of the paper substrate the diversity of possible spectral print reproduction was goal to be checked. The fact that in process of reaching final confirmation or negation of spectral print possibility many different steps are conducted it was very important to make that process decreased in time consumed. In this particular case there were 32 spectral data color samples given for which feasibility was to be checked. Nevertheless, that was just the subset of initial amount wanted to be reproduced in form of spectral print. For that reason the algorithm that enables the whole process, from spectral reflectance input to final decision of sending to printer or not, automated was proposed.

2. GARNAMENT PRODUCTS

Within this work focus was on feasibility of particular product. The collaboration with the retail store resulted in obtaining real samples and testing the possibility of spectral print reproduction with printer in our lab. The challenge was in trying to reduce the cost that retailer currently incur on one front of the retail color development process. That particularly involves recurring expenditure on 5 cm x 5 cm fabric samples that are produced to within 0.8 DE CMC. This is valid for illuminant UL3000 and 10 degrees observer. Designers use these physical representations when they are deciding which shade an item of garment product will be, or which shade needs to be placed near another in a printed or yarn dyed pattern on a garment product. The existing set of roughly 4000 colors is supporting the design process within the color set that designers are able to pick from. Once their colors for a season and brand are picked, 5cm x 5cm fabric samples are ordered to work with. The 4000 colors are supported using spectral data. That reference helps to keep the color on shade through many production runs, i.e. of color chips, of the color standards, and of the garments that are specified to be in close tolerance of these colors. With that given one set of spectral data for all colors, within scope of these thesis feasibility of printing particular colors out on as needed basis was tested. The possibility of printing these color samples versus purchasing them from a dyeing company would significantly save in cost per color. That is why the important step was focus on investigation the feasibility of being able to produce these colors accurately and consistently over the many variables that arise during consecutive runs. The starting issue in getting the print head create the wanted output, was to replace the D50 table with a UL3000 illuminant. The reason for that was the fact that color standards are made using reactive dyes, and the printers are limited to a significantly smaller set of colorants. Therefore, from a reflectance curve matching standpoint it was expected that there will likely be gaps. To overcome that problem the try to match to UL3000 illuminant was very important. Another challenge that was related to gamut is the difference in available chroma in the chromophores. Given that there are spectral data for all 4000 colors available, the brightest colors to be produced to produce are known as well but only the right combination of paper and colorants will create the maximum chroma. This is due to having the spectral data for the targets it would be easy to generate the L*,a*,b* C, and h values for all colors [2] [6]. From this step then it is possible to determine the maximum chroma needed. This would be a base ground for possible realization of coverage for given gamut [4] [7].

3. PROBLEM STATEMENT

What was done by now was the reproduction of the same set of 4000 colors using pigments in an injection molded process. Within that the knowledge that reflectance of colors made while using reactive dyes helped in match and use reflectance curves of pigments. That was why the whole process wanted to be moved to one step further - ink and paper combination. The samples used for our calculation were subset of original set consisted of 4000 samples. The subset consisted of 32 data samples. Spectral data of a textile standard and a plastic standard for the 10 degree observer weighted illuminant were given. The colors made by injection molding were used as color standards which suppliers in the hard goods area need to match. The idea was to have 'pre-translated' the color difference between textile dyes used in Apparel and Soft home products, and pigments used in Hard home areas. The main goal was to have the L*a*b* values of printed samples to match the L*a*b* values of the standard or have the color difference in terms of CMC DE in UL3000, which is store light, for 10 degree observer between the two be as low as possible [5]. An acceptable difference limit was defined with value of is 0.8 DE CMC. Those that fall outside of that difference up to 1.2 can be given special consideration by using visual determination of color difference. Those above 1.2 can be identified as out of gamut for the system under investigation. Spectral reflection data was obtained on spectrophotometer Datacolor SF600 Plus CT for each associated color. The values of reflectance were measured by this instrument at 10 nm interval starting at 400nm. Datacolor SF600 plus CT has an integrating sphere for illumination of the sample and the detector for the spectral analyzer is placed at 8 degrees from normal to the surface of the aperture plane (sample port). Sample ports are configurable depending on size of sample being presented. LAV (Large Area View) aperture plate is 30 mm illuminated and 26nm measured. This is important for ability to maximize the surface area to be measured which is ideal to measure color without regard to a textured surface.The instrument is dual-beam spectrophotometer with diffuse illumination and high black trap performance. The main metric that defines a difference measure used here is CMC.

$$\Delta E^*_{CMC} = \sqrt{\left(\frac{L^*_2 - L^*_1}{lS_L}\right)^2 + \left(\frac{C^*_2 - C^*_1}{cS_C}\right)^2 + \left(\frac{\Delta H^*_{ab}}{S_H}\right)^2} \quad (1)$$

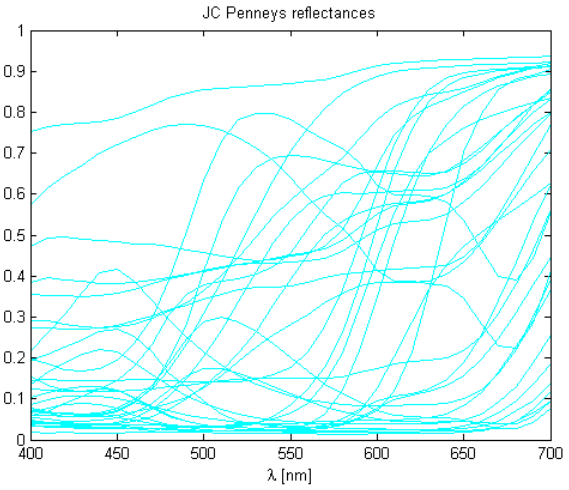

Figure 1: Spectral reflectances of 32 color samples.

Figure 2: Lab values of color samples.

4. EXPERIMENT

The twelve channel HP DesignJet Z3200 printer was employed in experiment.Having available that strong printing machine was crucial element because of its much better gamut size comparing to the four channel printers. The gamut of the HP DesignJet Z3200 printer was obtained for five different papers and visualized using ICC3D [**?**] Calibration process of the HP DesignJet Z3200 printer results with a printed color chart made of a ramps for each channel. These ramps were then measured manually with spectrophotometer because of the specific hexagonal shape of color patches.

5. ALGORITHM

We present the state-of-the art algorithm for making this process automated. At the beginning of the proposed algorithm the input data required was the spectral reflectance data measurements. It needs to be noted here that it is important take care of the geometry o measurements for the main goal. When (if) spectral print reproduction of wanted object was confirmed to be feasible the final print reproduction should be measured under same conditions, geometry and illuminats. Since the next step was mapping the color gamut of a initial values to the gamut given by output mechanism, printer, the values were represented with an image. For the image format Tagged Image File Format was chosen. TIFF image format enables data obtained from spectral reflectances measured under certain illuminant to be presented separately for each of L*, a* and b* channels. If this wanted to be replaced with CMYK values TIFF is again the best choice because in that case it represents four channels separately. By use of TIFF format the conversion to RGB space was skipped, regarding important use of displays, during the whole process.This helps in making the whole process faster and simple. After the TIFF image was created in CIELAB color space next step was to map that image file, which is the representation of the spectral reflectance of the object wanted to be printed, to the gamut of a printed for a certain paper. In process of mapping, ICC3D software was employed and constrains set was minimum delta and constant hue in order to achieve the best perceptual match of final reproduction. Obtained mapped image is again in TIFF format which enables to extract the L*, a* and b* channel data. Next, that data was used in step of comparing the differences between the initial TIFF image and mapped TIFF image [1]. Then the calculation of the differences for several color spaces in case of several paper substrates under different illuminants was done. Visualization of the points that are out of gamut for a certain paper was presented in order to be able to notice which part of gamut should be considered to be extended if possible was the next step done. Finally, with the constraints to be considered, i.e. value more than 1.2 for delta CMC overcomes the aim, the spectral color points were confirmed or not to be feasible to print within the gamut possibilities for specific combination of colorants/paper of printer given. The feasibility of the defined input data from retailer was then tested with this proposed method for five different papers. The scheme can be seen in fig. 3.

6. RESULTS

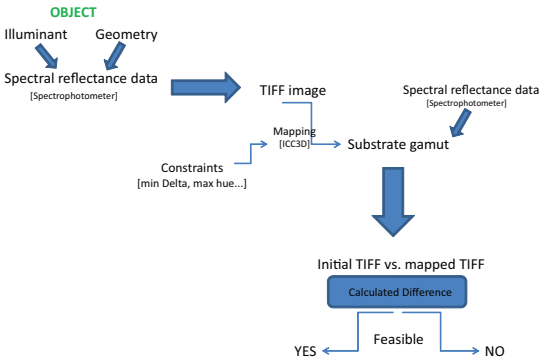

Figure 3: Feasibility of spectral print reproduction algorithm scheme.

With given constraints of the error allowed within delta CMC value 0.8 the process of spectral color reproduction was decided to be started with checking the feasibility. Two printers that were used for spectral print modeling were considered to be employed, Xerox Phaser 6250 color laser and Oce ColorWave 600 printer. The process was started with numerical and visual representation of their gamuts. This was done by using color ramps of separated printed colorants. Next, spectral reflection data of ramp was measured with and finally represented with the L*a*b* values by means ICC3D software. The functionality of the ICC3D software is the ability to read color data as an image in some standard format or that are extracted by the gamut tag of an ICC profile [3]. It also enables the color data to be displayed in different ways in various 3D color spaces. This is very useful for visualizing the whole process of checking the spectral print feasibility. The L*a*b* values of the four channels printer and their gamuts are shown with fig. 4 for Xerox Phaser 6250 and fig. 4 for the Oce ColorWave 600 printer.

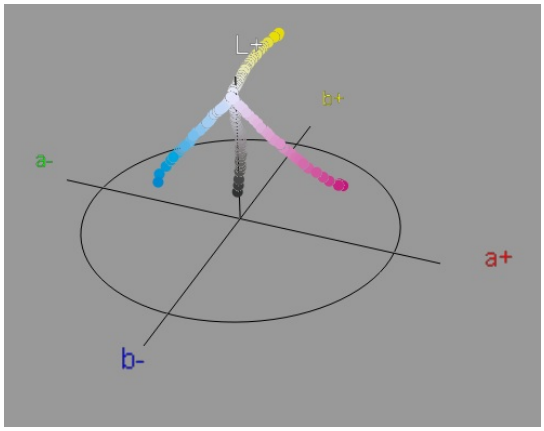

Figure 4: 3D gamut visualization of Xerox Phaser 6250 printer is shown on the right side. On the left side L*a*b* values of ramp printed separately for all four channels is presented.

Five different papers were employed in obtaining results: HP Heavy Coated paper $(130g/m^2)$, HP Professional Matte Canvas $(430g/m^2)$, HP Artist Matte Canvas $(380g/m^2)$, HP Universal Coated Paper $(95g/m^2)$ and HP Recycled Bond Paper $(80g/m^2)$. After applying proposed algorithm the best results were obtained for the HP Artist Matte Canvas and the worst was given with gamut of HP Recycled Bond Paper used as substrate.

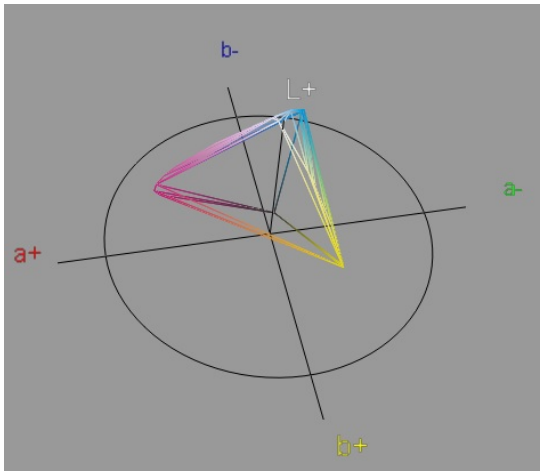

Figure 5: 3D gamut visualization of Xerox Phaser 6250 printer is shown on the right side. On the left side L*a*b* values of ramp printed separately for all four channels is presented.

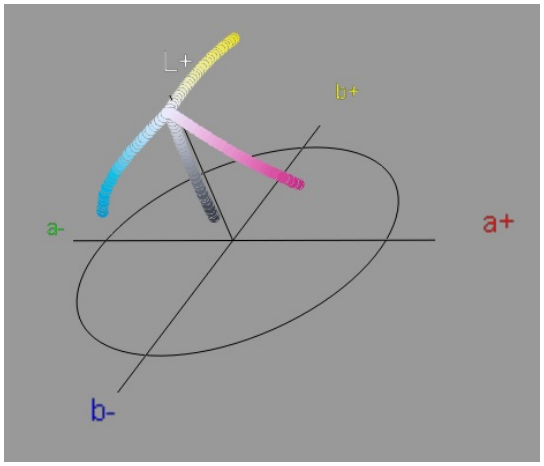

Figure 6: 3D gamut visualization of Oce ColorWave 600 printer is shown on the right side. On the left side L*a*b* values of ramp printed separately for all four channels is presented.

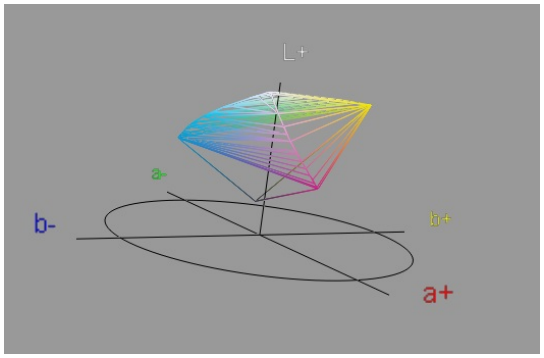

Figure 7: 3D gamut visualization of Oce ColorWave 600 printer is shown on the right side. On the left side L*a*b* values of ramp printed separately for all four channels is presented.

6.1 HP Artist Matte Canvas

The HP Artist Matte Canvas is $380g/m^2$ paper often for fine art reproduction. This paper was chosen for the texture that resembles even more to the cloth that the HP Professional Matte Canvas.In this particular case of paper it can be seen from the fig. 8 that the maximum CMC differnece is obtained under illuminnat UL3000 so in comparisment with the rest illuminants the calculations obtained are satisfied. This is in case of minimum but if the average is to be read, the 1.8 and 0.8 threshold values become overpassed. This is again, as mentioned before, misleading number because the significant amount of samples is still above 1.2 values and 0.8. This can be seen from the histogram in fig. 9. From there is easier to observe the amount of samples that are feasible to be produced in spectral print reproduction, in particular 20 samples are under CMC 0.8 value and 5 under CMC 1.2 value of total 32 samples. In observing the values that go over the 1.2 CMC value, the particular color points that are the most far away from wanted values to be mapped are in yellow and dark blue(black) part of the color gamut that can be seen from the fig. 10. From here the lead to direction to look for gamut extension in order to achieve the wanted spectral reproduction is created.

C	HP Artist Matte Canvas											
	ΔE			Δ94			ΔCMC			ΔE00		
	min	max	avg	min	max	avg	min	max	avg	min	max	avg
D50	0,21	11,02	2,45	0,11	10,49	1,96	0,13	18,77	2,73	0,10	7,54	1,57
D65	0,21	10,65	1,91	0,11	10,11	1,56	0,13	18,07	2,39	0,13	7,25	1,26
A	0,21	11,02	2,47	0,11	10,49	1,97	0,13	17,05	2,73	0,10	7,54	1,58
C	0,21	11,04	2,47	0,11	10,50	1,97	0,13	17,77	2,73	0,10	7,50	1,58
F2	0,21	11,02	3,31	0,20	10,49	2,50	0,28	18,77	3,19	0,21	7,54	2,02
UL3000	0,21	10,28	1,93	0,11	9,72	1,57	0,13	17,37	2,36	0,10	6,96	1,27

Figure 8: Results of gamut mapping to paper C given with different color differences equations under 6 illuminants.

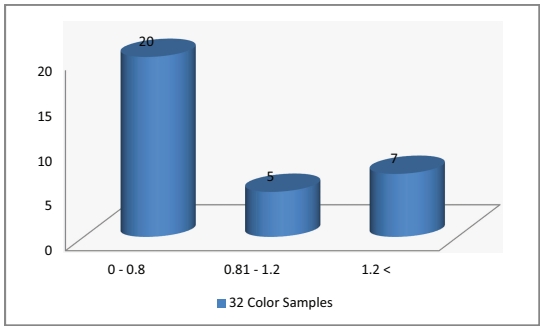

Figure 9: Histogram of resulting CMC difference for 32 color samples mapped to printer gamut on paper C.

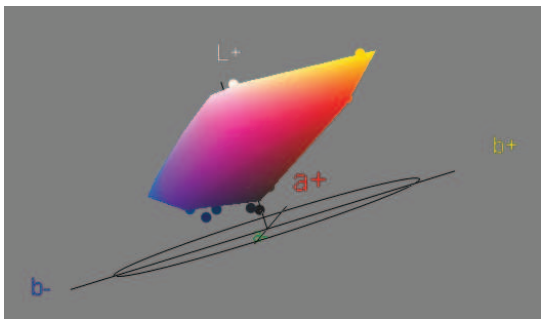

Figure 10: Visualization of initial color values and gamut of print created with paper C before mapping, in 3D space.

Again, starting from the intimal 3 separated channels in TIFF format the mapped version to gamut obtained on HP Artist Matte Canvas is created and presented visually with L*a*b* values in color ramp of target colors with the fig. 11

Figure 11: Color samples mapped to gamut of HP Artist Matte Canvas under illuminant UL3000 for 10 degree observer.

6.2 HP Recycled Bond Paper

The HP Recycled Bond Paper is $80g/m^2$ paper often for low print reproduction. This paper was chosen for establishing the relation between specific requirements with the paper substrate supporting the green technologies.This was to check the results with taking into account the future possibility of spectral print reproduction on reused paper substrate and in that way making it more affordable and desirable for environment.In this particular case of paper it can be seen from the fig. 12 that the maximum CMC differnece is obtained under illuminnat UL3000 so in comparison with the rest illuminants the calculations obtained are satisfied. This is in case of minimum but if the average is to be read, the 1.8 and 0.8 threshold values become overpassed. This is again, as mentioned before, misleading number because the significant amount of samples is still above 1.2 values and 0.8. This can be seen from the histogram in fig. 13. From there is easier to observe the amount of samples that are feasible to be produced in spectral print reproduction, in particular 7 samples are under CMC 0.8 value and 3 under CMC 1.2 value of total 32 samples. From these results it can be concluded that quality of the paper strongly affects the feasibility of the spectral print reproduction. In observing the values that go over the 1.2 CMC value, the particular color points that are the most far away from wanted values to be mapped are in yellow and dark blue(black) part of the color gamut that can be seen from the fig. 14. From here the lead to direction to look for gamut extension in order to achieve the wanted spectral reproduction is created.

E	HP Recycled Bond paper											
	ΔE			Δ94			ΔCMC			ΔE00		
	min	max	avg	min	max	avg	min	max	avg	min	max	avg
D50	0,26	22,44	7,82	0,21	19,70	5,23	0,28	34,64	6,74	0,25	14,98	4,30
D65	0,26	22,56	7,86	0,21	19,32	5,17	0,28	33,95	6,66	0,25	14,67	4,25
A	0,26	24,48	8,53	0,21	19,83	5,58	0,28	34,71	7,13	0,25	15,17	4,62
C	0,26	22,11	7,64	0,21	19,32	5,06	0,28	33,95	6,55	0,25	14,67	4,16
F2	0,26	30,78	10,09	0,24	18,41	6,15	0,33	32,47	7,61	0,29	14,07	5,10
UL3000	0,26	22,57	7,57	0,21	18,79	5,06	0,28	33,16	6,54	0,25	14,38	4,16

Figure 12: Results of gamut mapping to paper E given with different color differences equations under 6 illuminants.

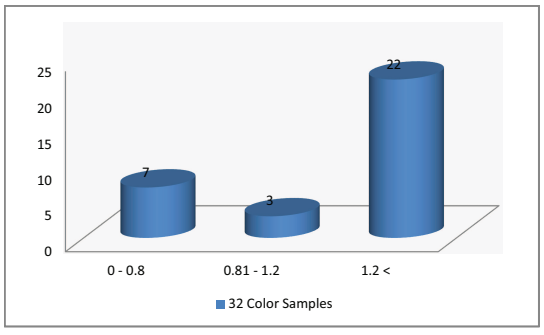

Figure 13: Histogram of resulting CMC difference for 32 color samples mapped to printer gamut on paper E.

Starting from the intimal 3 separated channels in TIFF format the

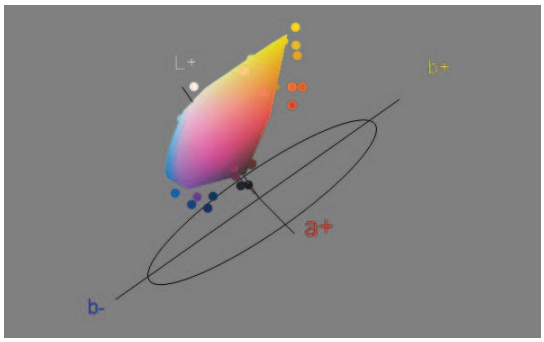

Figure 14: Visualization of initial color values and gamut of print created with paper E before mapping, in 3D space.

mapped version to gamut obtained on HP Artist Matte Canvas is created and presented visually with L*a*b* values in color ramp of target colors with the fig. 15

Figure 15: Color samples mapped to gamut of HP Recycled Bond Paper under illuminant UL3000 for 10 degree observer.

7. ANALYSIS OF THE RESULTS

After all substrates were tested and the feasibility was given with the results obtained the comparison of the five papers was done. This can be seen from the histogram in fig. 16. The fact that calculating the average difference from the ramp of target set of colors to be spectrally reproduced is not giving the correct answer need to be noted. For that reason histogram representation was used for more thorough conclusions about the feasibility. This move brings the improvement to visual representation of the data as well as to the calculation results. Finally, all of the mapped values are given

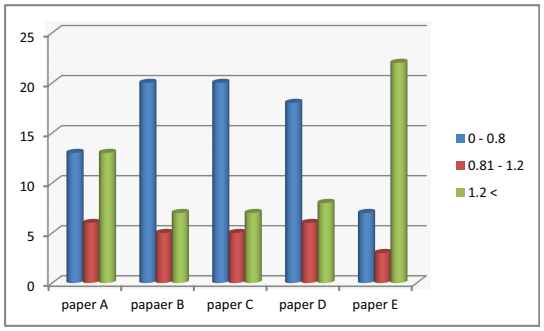

Figure 16: Histogram of resulting CMC difference for initial 32 color samples mapped to printer gamut on papers A,B,C,D and E.

with the L*a*b* values that are possible to be reproduced. Observing it carefully gives the opportunity to apply the 3 visualization of gamuts to real samples wherease the wanted extention of gamut in yellow and blue (black) direction of gamut space is as well noticed from fig. **??**. If focused on the yellow and blue samples of given ramp the deviation from the initial ramp can be seen even with the bare eye. It is somewhat more difficult to noticed yellow mapped samples difference that blue ones due to ability of human visual system.

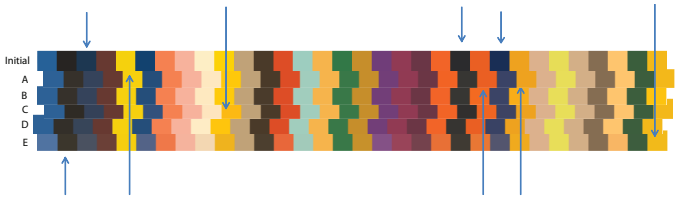

Figure 17: Color samples mapped to gamut of five different papers under illuminant UL3000 for 10 degree observer. The arrows point the samples most affected with the gamut mapping. Initial L*a*b* values are given in top ramp followed by papers A,B,C,D,and E towards the bottom. The arrows point the samples most affected with the gamut mapping.

8. CONCLUSION

We presented a more way of checking the possibility weather the certain object and its spectral reflectance data can be printed or not satisfying certain allowed deviations of the perfect spectral match. The new algorithm for making the whole process saving time was proposed. This is due to including all the segments of the process into one code. For this particular case the results have shown feasibility of spectral print reproduction more more than half of the input data given. The lack was noticed in yellow and blue regions of the gamut. This is area to be taken into consideration while adding or changing different colorants. The goal was to make the process of deciding on feasibility automated for bigger amount of input data in order to help the whole process of spectral printing be more efficient and simple.

9. ACKNOWLEDGMENTS

We want to thank the Norwegian Color and Media Computing Laboratory for providing the resources for the research and retailer store for providing us with samples and data. We also thank European Commission for funding Color in Informatics and Media Technology (CIMET) masters program.

10. REFERENCES

[1] Adobe photoshopő tiff technical notes.
[2] *Hunter l,a,b Color Scale*.
[3] I. Farup and J. Y. Hardeberg. Interactive color gamut mapping.
[4] H. Kipphan. *Handbook of Print Media: Technologies and Production Methods*. 2001.
[5] H. B. Nicolas Bonnier, Francis Schmitt and S. Berche. Evaluation of spatial gamut mapping algorithms.
[6] P. D. B. Roy S. Berns, Francisco H. Imai and D.-Y. Tzeng. Multi-spectral-based color reproduction research at the munsell color science laboratory.
[7] L. A. T. Yongda Chen, Roy S. Berns. Extending printing color gamut by optimizing the spectral reflectance of inks.